



THE UNIVERSITY *of* EDINBURGH

Edinburgh Research Explorer

Towards the development of a probabilistic approach to informal settlement fire spread using ignition modelling and spatial metrics

Citation for published version:

Cicione, A, Gibson, L, Wade, C, Spearpoint, M, Walls, R & Rush, D 2020, 'Towards the development of a probabilistic approach to informal settlement fire spread using ignition modelling and spatial metrics', *Fire*, vol. 3, no. 4, 67. <https://doi.org/10.3390/fire3040067>

Digital Object Identifier (DOI):

[10.3390/fire3040067](https://doi.org/10.3390/fire3040067)

Link:

[Link to publication record in Edinburgh Research Explorer](#)

Document Version:

Peer reviewed version

Published In:

Fire

General rights

Copyright for the publications made accessible via the Edinburgh Research Explorer is retained by the author(s) and / or other copyright owners and it is a condition of accessing these publications that users recognise and abide by the legal requirements associated with these rights.

Take down policy

The University of Edinburgh has made every reasonable effort to ensure that Edinburgh Research Explorer content complies with UK legislation. If you believe that the public display of this file breaches copyright please contact openaccess@ed.ac.uk providing details, and we will remove access to the work immediately and investigate your claim.



1 Article

2 Towards the development of a probabilistic approach 3 to informal settlement fire spread using ignition 4 modelling and spatial metrics

5 Antonio Cicione ^{1,*}, Lesley Gibson ², Colleen Wade ³, Michael Spearpoint ⁴, Richard Walls ⁵ and
6 David Rush ⁶

7 ¹ Department of Civil Engineering, Stellenbosch University, Stellenbosch, South Africa; acicione@sun.ac.za

8 ² School of Engineering, University of Edinburgh, Edinburgh, UK; Lesley.gibson@ed.ac.uk

9 ³ Fire Research Group Ltd, New Zealand; colleen.wade@fireresearchgroup.com

10 ⁴ OFR Consultants, Manchester, UK; michael.spearpoint@ofrconsultants.com

11 ⁵ Department of Civil Engineering, Stellenbosch University, Stellenbosch, South Africa; rwalls@sun.ac.za

12 ⁶ School of Engineering, University of Edinburgh, Edinburgh, UK; d.rush@ed.ac.uk

13 * Correspondence: acicione@sun.ac.za

14 Received: date; Accepted: date; Published: date

15 **Abstract:** Large conflagrations of informal settlements occur regularly leaving thousands of people
16 homeless daily and taking tens of thousands of lives annually. Over the past few years a large
17 amount of data has been collected from a number of full-scale informal settlement fire experiments.
18 This paper uses that data with a semi-probabilistic fire model previously proposed by the authors,
19 to illustrate the potential applications of the fire spread method proposed. The current model is
20 benchmarked against a 20 dwelling full-scale informal settlement fire experiment, and the effects of:
21 a) the ignition criteria; b) wind direction; and c) wind speeds, on the predicted fire spread rates are
22 investigated through the use of a parametric study. Colour maps of the fire spread rates and patterns
23 are then used to visually interpret the effects of different types of fire scenarios and fire breaks.
24 Finally, the fire spread capability within B-RISK is used to derive a linear equation for the potential
25 fire spread rate as a function of the settlement spatial metrics (e.g. density and distance to nearest
26 neighbour). To further illustrate the potential application of this work, the fire spread rate equation
27 is then applied across the whole of Cape Town, South Africa to show the 10 informal settlement
28 areas most at 'risk' of large conflagrations.

29 **Keywords:** informal settlements; fire spread; ignition; spatial metrics; B-RISK; probabilistic
30 simulation
31

32 1. Introduction

33 Informal settlements, also known as shantytowns or slums, are settlements that are typically not
34 formally planned and consist of makeshift structures built on land that has not been designated for
35 residential use. These structures, more commonly known as shanties, shacks or informal settlement
36 dwellings (ISDs), are typically built from materials that are immediately available in the inhabitants'
37 surroundings, many of which are combustible. Informal settlements are extremely vulnerable to large
38 conflagrations as a result of these combustible structures coupled with the close proximity at which
39 these dwellings are built and prevailing weather conditions.

40 In South Africa alone there are more than 5000 ISD fires per annum, and the number of fires are
41 increasing annually [1]. According to the World Health Organization (WHO), fires cause
42 approximately 180,000 deaths globally per annum, with the majority of those deaths and associated

43 burn injuries occurring in low- and middle-income countries [2]. Figure 1 depicts a fire that occurred
44 in 2016 in the Estrada de Alpina favela of Sao Paulo, Brazil, which destroyed hundreds of informal
45 homes [3]. Figure 2 depicts a fire that occurred in 2017 in the Imizamo Yethu informal settlement in
46 Hout Bay, South Africa, which destroyed more than 2100 homes and left approximately 9700 people
47 homeless [4].



Figure 1. Fire in the Estrada de Alpina favela of Sao Paulo [3]



Figure 2. Imizamo Yethu informal settlement fire [4].
[With permission from Ryan Heydenrych](#)

48 The study of informal settlement fires is a relatively new research field. Previous research has
49 set out to better understand ISD enclosure fire dynamics (individual scale) and informal settlement
50 fire dynamics (macro scale). A number of large-scale ISD experiments have been conducted [5–9],
51 ranging from single dwellings to 20 dwellings in a single burn. In previous work, simulations using
52 Fire Dynamics Simulator (FDS) have been undertaken to demonstrate the software’s ability to predict
53 the fire behaviour of single dwelling fires [7]. However, these comprehensive simulations took weeks
54 to run on the High Performance Computer of Stellenbosch University, which made it impractical to
55 run scenarios consisting of multiple dwellings. Cicione *et al.* [6] proposed some simplifications that
56 were incorporated into those FDS simulations, which significantly reduced the computational time
57 needed to run the multiple dwelling cases. However, the simplified simulations were found to be
58 extremely sensitive to input parameters and, although the simplifications reduced the computational
59 ~~time-needed~~[requirements](#), the time needed to simulate entire settlement scenarios would still be
60 impractical.

61 As an alternative, Cicione *et al.* [10] have developed a preliminary semi-probabilistic model of
62 informal settlement fire spread using B-RISK (a two-zone fire modelling software tool). The aim was
63 to take the first step towards developing a tool that could assist authorities of countries with large
64 informal settlements to provide predictive capabilities that can help in identifying high risk areas or
65 quantify the magnitude of an incident to which municipalities may need to respond. The semi-
66 probabilistic modelling approach [10] showed promising results compared to a triple ISD experiment
67 and to the Imizamo Yethu informal settlement fire that occurred in 2017. In order to capture more
68 realistic fire spread behaviour that occurs in settlements due to their high variability, the ISDs should

69 not only be randomly selected based on floor area (as done by Cicione *et al.* [10]), but also based on
70 the cladding/lining material (as discussed in this paper) and their expected heat release rates.

71 Using spatial analysis with Geographic Information Systems (GIS), the layout of informal
72 settlements and the spatial arrangement of individual dwellings relative to each other (referred to as
73 spatial metrics) have been postulated to be indicative of fire spread risk. Identified fire spread risk
74 spatial metrics can then be applied to settlements so that those most at risk of fire spread can be
75 identified. For example, Gibson *et al.* [11] used burn areas identified from satellite imagery to
76 empirically obtain spatial metric values of settlements from their dwellings within the burn areas.
77 Settlements with similar spatial metric values were then identified within a broader environment and
78 were postulated to be at a high risk of fire spread. This approach relies on threshold values (75th
79 percentile values of spatial metrics found in the burn areas) to identify either settlements which are
80 at higher risk of fire spread or those which are not. This binary approach is simplistic, where in reality
81 all settlements are at some risk of fire spread and thus a more nuanced, fire science-based approach,
82 is needed.

83 It is with this backdrop that this paper seeks to:

- 84 1. Further investigate the semi-probabilistic model of informal settlement fire spread using B-
85 RISK, as proposed by ref. [10] by:
 - 86 a. investigating the effect of the ignition properties (i.e. the Flux-Time Product (FTP) index,
87 FTP value and the critical heat flux (CHF)) assigned to ISDs in B-RISK, by comparing the
88 simulation results to a full-scale 20 dwelling informal settlement fire experiment [8];
 - 89 b. post-processing the B-RISK time-to-ignition output data, to plot colour maps of the fire
90 spread rates of the settlement under consideration, allowing end users to better interpret
91 the results;
- 92 2. Derive an equation for potential fire spread rate as a function of the settlement spatial metrics
93 by:
 - 94 a. applying the semi-probabilistic approach using B-RISK (i.e. randomly populating different
95 informal settlement scenarios) to determine which spatial metrics (i.e. dwelling density,
96 edge density, etc.) pose the highest risk to informal settlement fire spread, which are then
97 used to derive a fire spread rate equation;
 - 98 b. applying the equation to all informal settlements across the whole of Cape Town to identify
99 the ten, larger than 1 ha, most at risk of fire spread, based on this semi-probabilistic
100 approach.

101 2. Radiation and ignition of secondary items in B-RISK

102 B-RISK is a two-zone model [12] that is typically used to simulate fire and smoke within
103 enclosures bounded by walls and ceilings. B-RISK calculates the ignition of secondary items as a
104 result of radiation from either one or more burning items or from the hot gas layer within the
105 enclosure. This section gives a brief review of the radiation and ignition submodels employed in B-
106 RISK but for more information ~~regarding the model~~, the reader should refer to the user guide and
107 technical manual [13]. The radiation heat transfer method employed by B-RISK has been studied in-

108 depth and has been found to be a suitable method for a variety of cases. Sazegara et al. [14]
 109 benchmarked the single item ignition prediction capability of B-RISK using results from the furniture
 110 calorimeter against room-size experiments. The method has also showed promise in other fields e.g.
 111 Tohir and Spearpoint [15] made use of this method to have simulated the BRE multiple vehicle fire
 112 spread experiment [16].

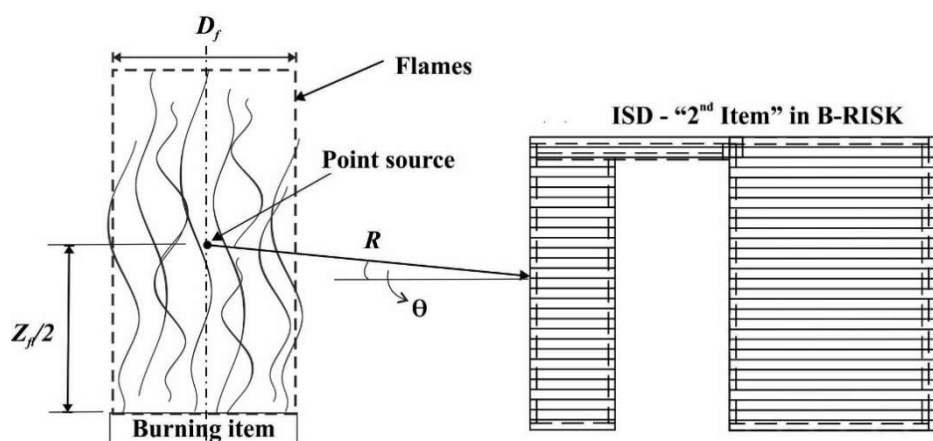
113 In this work, the item-to-item submodel of B-RISK is used to simulate fire spread between ISDs,
 114 which is a novel application for which the software was never originally designed for. To simulate
 115 spread between ISDs in B-RISK, the dwellings are simplified to items (as in ref. [10]) and treated as
 116 being 'outside', with the settlement being simplified to a 'room' that is fully open (i.e. a room with 5
 117 vents the size of the room boundaries to allow all the hot gases to escape to the 'outside'). This
 118 effectively removes the 'zone' element from the zone model, but by keeping the radiation and ignition
 119 submodels, which is a convenient means of using these submodels rather than recreating them from
 120 scratch as a standalone tool. In this easepaper, the same approach is followed. Hence, there will be
 121 no hot layer build up and the focus will be on item-to-item ignition (in other words, ISD-to-ISD fire
 122 spread).

123 2.1. Radiation

124 B-RISK (version 2019.043) employs the Point Source Method (PSM) in the Design Fire Generator
 125 (DFG) submodel as its default flame radiation model and this can be described mathematically with
 126 the following equation [13]:

$$127 \quad \dot{q}_f'' = \frac{\dot{Q}\chi_r \cos\theta}{4\pi R^2} \quad (1)$$

128 where \dot{q}_f'' is the radiant heat flux, measured in kW/m², received by the target item from the flaming
 129 burning item; \dot{Q} is the total heat release rate, measured in kW, of the burning item; χ_r is the
 130 radiative fraction; θ is the angle between the radial distance (R) and an imaginary line parallel to the
 131 floor where R intersects with the target item, as depicted in Figure 3; and R is the radial distance,
 132 measured in metres, from the centre of the flaming region of the burning item to the nearest point of
 133 the target item. Figure 3 depicts the geometry assumed in this paper and also visually illustrates the
 134 variables used in Equation 1. In the B-RISK implementation R will always be the plan view distance
 135 so that theta will be zero.



136

137 **Figure 3.** PSM geometry between burning and target items [10]. Used with permission from Elsevier.

138 Since the flames from a real burning ISD issue from door and window openings in addition to
 139 flames that develop through the roof of the structure, the fire is assumed to originate from the base
 140 of the ISD for the PSM. The flame height z_{fl} (Figure 3), measured in metres, is calculated using
 141 Heskestad's [17] flame height correlation given by the following formula:

142
$$z_{fl} = 0.235\dot{Q}^{2/5} - 1.02D_f \tag{2}$$

143 where D_f is the width of the burning item [m]. Cicione et al. [10] added the functionality to B-RISK
 144 to account for the effects of wind, by updating the radial distance R to R' , where R' is calculated as
 145 follows (refer to Figure 4):

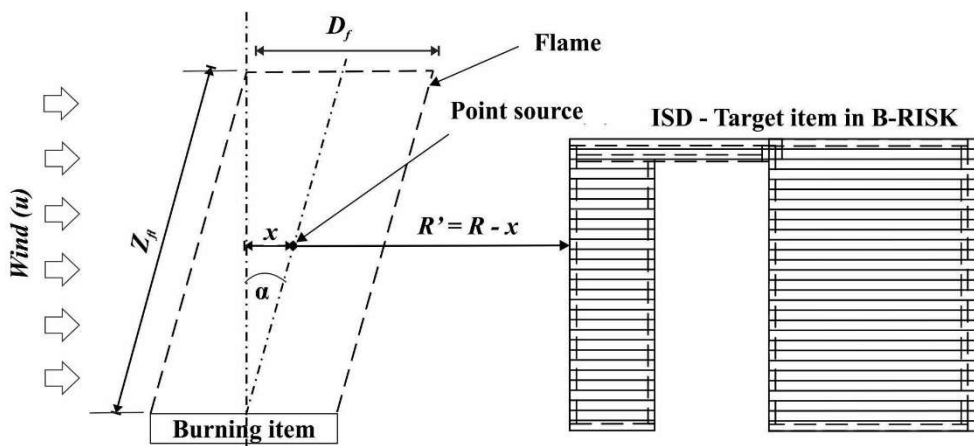
146
$$R' = R - \frac{z_{fl}}{2} \cdot \sin \alpha \tag{3}$$

147 where α is the angle between the vertical line from the centre of the burning item to the intersection
 148 of the wind-tilted flame axis and is calculated as follows [18]:

149
$$\tan \alpha = 2.73Fr^{2/5} \cdot Q^{*-0.1(1+2.5y)} \cdot \left(\frac{W}{r^*}\right)^{-0.5} \tag{4}$$

150 where Fr is the Froude number given by u^2/gD_f (where u is the wind speed [m/s] and is assumed
 151 to be constant through the height of the domain and that it is not affected by the terrain or the items,
 152 D_f is the short length of the rectangular burning item [m] and g is the acceleration due to gravity
 153 [m/s²]); Q^* is the dimensionless heat release rate given by $\dot{Q}/(\rho_a C_p T_a g^{1/2} D^{5/2})$ (where \dot{Q} is the
 154 heat release rate [kW], ρ_a is the density of ambient air [kg/m³], C_p is the specific heat at constant
 155 pressure [kJ/(kg·K)] and T_a is the ambient temperature [K]); $y = 2$ for $0.05 < Q^* < 0.38$ and $y = 2/3$ for
 156 $0.38 < Q^* < 12.8$; W is the long length of the rectangular burning item, and $r^* =$
 157 $\sqrt{\text{burning item floor area}/\pi}$.

158



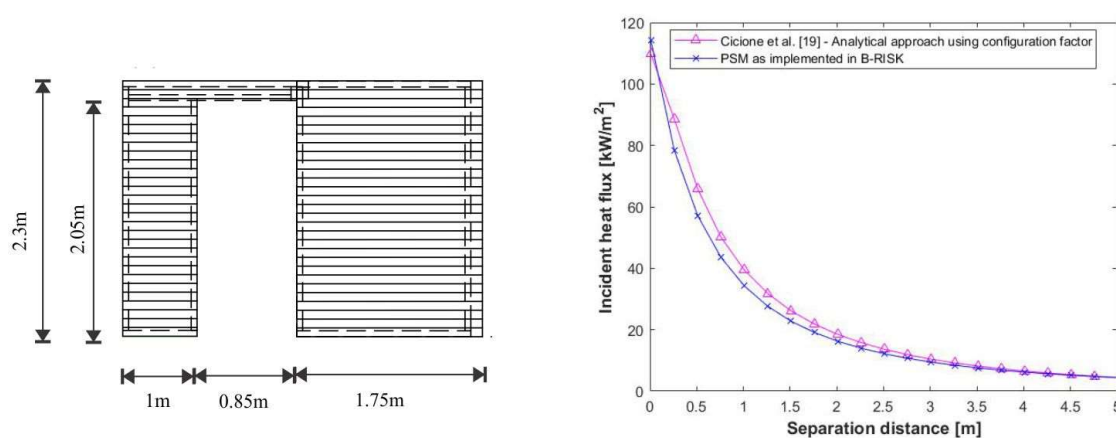
159

160 **Figure 4.** PSM geometry between burning and target items with wind effects [10]. [Used with permission from](#)
 161 [Elsevier.](#)

162 Treating the ISDs as items and calculating the radiation emitted using the PSM (meaning an item
 163 can burn and flame from all sides equally) as employed by B-RISK is a simplification of reality. A
 164 fundamentally more correct method to calculate the incident radiation at a distance from a dwelling
 165 should consider the configuration factor of the actual wall geometry of the dwelling emitting the heat,
 166 such that:

$$\dot{q}_{inc}'' = \sigma \phi \varepsilon T^4 \quad (5)$$

167 where σ is the Stefan-Boltzmann constant [5.67×10^{-11} kW/($m^2 K^4$)], ϕ is the configuration factor
 168 between the emitter and target surface, ε is the emissivity of the emitter, and T is the temperature
 169 of the emitter [K]. Each wall of the ISD will thus have a different emitted incident heat flux based on
 170 the setup-arrangement of the wall (e.g. a wall with a window opening will radiate more heat-energy
 171 compare to a wall with no openings). The radiation emitted from ISDs ~~are-is~~ discussed on a
 172 fundamental level in ref. [19]. If a worst case scenario is assumed (i.e. being conservative in this case),
 173 which will be the radiation in front of a door opening based on the findings from ref. [19], the
 174 radiation estimate can be calculated using the PSM and compared using-to the fundamental analytical
 175 approach (Equation 5), which gave good correlation to the measured full-scale ISD experimental
 176 results, ~~to the PSM implemented by B-RISK~~. Consider the scenario on the left in Figure 5, i.e. the exact
 177 scenario of the experiment conducted by ref. [19] which then corresponds to the radiation versus
 178 distance curve on the right, which was calculated by ref. [19] using Equation 5. ~~Should-Where~~
 179 the radiation versus distance ~~be-is~~ calculated using Equation 1, as implemented by B-RISK, the separation
 180 distance ~~would-is~~ be R minus half the width of the dwelling, χ_r ~~would-can be taken as~~ be 0.3 for
 181 timber cribs ~~as taken~~ from Table 3-4.14 of the SFPE Handbook [20], and \dot{Q} the maximum measured
 182 heat release rate of 7 MW [19], the curve in Figure 5 is obtained. Thus from Figure 5, the correlation
 183 between the simplified method implemented in B-RISK and the analytical method as implemented
 184 by ref. [19] has a maximum deviation of 11.5% at a distance of 0.26 m.
 185



186
 187 **Figure 5.** Comparison of the radiation emitted from ISD as calculated using the PSM and Equation 5 (refer to
 188 ref. [19] for more details on the analytical method)

189 It should however be noted that should Equation 5 be applied to a wall scenario with no
 190 openings, the radiation emitted would be significantly less compared to the PSM (the radiation versus
 191 distance would remain the same for the PSM), but since fire spread is assumed to occur at the point
 192 where the radiation is the highest, the PSM is sufficient for the intended use in this paper.

193 2.2. Ignition

194 Currently, B-RISK employs the Flux-Time Product (FTP) method as its default ignition
 195 submodel. The FTP method is a simplified approach to estimate the time-to-ignition of a combustible
 196 item subjected to an incident heat flux. Shields *et al.* [21] generalized the FTP method such that:

$$197 \text{ FTP} = t_{ig}(\dot{q}_f'' - \dot{q}_{cr}'')^n \quad (6)$$

198 where t_{ig} is the time-to-ignition [s]; \dot{q}_f'' is the incident heat flux emitted by the burning item; \dot{q}_{cr}'' is
 199 the critical heat flux of the target item [kW/m²]; and n is known as the FTP index. The values for
 200 FTP , n and \dot{q}_{cr}'' are determined by conducting a number of ~~cone calorimeter ignition~~ experiments, at
 201 different incident heat fluxes, and plotting the range of $1/t_{ig}^{1/n}$ values against the corresponding
 202 incident heat fluxes, and iteratively varying n to obtain the trendline with the highest correlation
 203 coefficient (R^2), where the gradient of the trendline is equal to $FTP^{1/n}$ and the point of intersection
 204 with the y-axis is equal to \dot{q}_{cr}'' .

205 Piloted ignition measurements from the cone calorimeter for a variety of common lining and
 206 cladding materials used in informal settlements are available in refs. [22,23]. In this case, piloted
 207 ignition is assumed since ISDs are typically closely spaced [24,25] (especially the many dense
 208 settlements in Cape Town, and experiments considered in this paper, although this is not always the
 209 case) so ignition is often assumed to be by means of flame impingement [9]. Assuming piloted
 210 ignition also accounts for the effects of wind tilting flames and causing channelling between ISDs.
 211 Using Equation 6 and the cone calorimeter data, Figure 6 has been constructed where the FTP , n and
 212 \dot{q}_{cr}'' values for a number of these common lining and cladding materials used in informal settlements
 213 have been obtained, and are presented in Table 1.

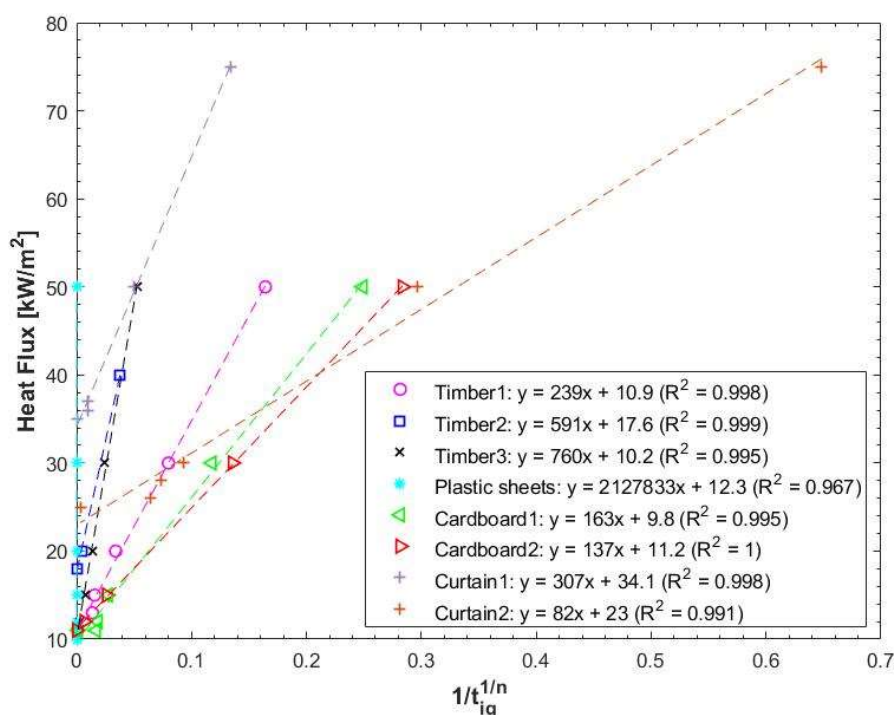
214 **Table 1.** FTP , n and \dot{q}_{cr}'' values for a number of these common lining and cladding materials used in informal
 215 settlements.

Item	FTP value [kW/m ²] ⁿ	FTP index (n)	Critical heat flux (\dot{q}_{cr}'') in kW/m ²
Timber 1	6394.5	1.6	10.9
Timber 2	2116.9	1.2	17.6
Timber 3	2866.0	1.2	10.2
Plastic sheets	18.4	0.2	12.3
Cardboard 1	1251.7	1.4	9.8
Cardboard 2	224.5	1.1	11.2
Curtain 1	97.6	0.8	34
Curtain 2	1145.5	1.6	23

216

217 It should be noted that the FTP values, FTP indexes and the critical heat flux (CHF) values
 218 obtained in Table 1 are based on data from piloted cone calorimeter experiments. Hence, these values
 219 are only applicable for piloted ignition scenarios, as assumed in this paper, and does not hold true
 220 for cases where a piloted source is not present. Baker *et al.* [26] developed an empirical approximation
 221 that can be used to update the FTP index, FTP value and the CHF for auto-ignition scenarios, where
 222 they assumed that the time-to-ignition for the piloted- and auto-ignition modes will converge at an
 223 incident flux of $\dot{q}_f'' = 120$ kW/m².

224



225

226

227

Figure 6. Correlation of ignition times and incident heat flux. t_{ig} is the time-to-ignition in seconds (cone calorimeter data from [ref. \[23\]](#))

228

3. Twenty-dwelling experiment versus B-RISK

229

230

231

232

233

In this section the B-RISK ISD fire spread method proposed by [ref. \[10\]](#) is benchmarked against a full-scale 20 dwelling experiment [8]. A parametric study of the effect of a) wind speed, b) wind direction, and c) ignition criteria, on fire spread rates is then conducted by only changing one variable of the 20 dwelling benchmarked simulation (baseline simulation) and comparing it to the baseline simulation and the other baseline variants.

234

235

3.1. Experimental and numerical model setup

236

237

238

239

240

241

242

243

244

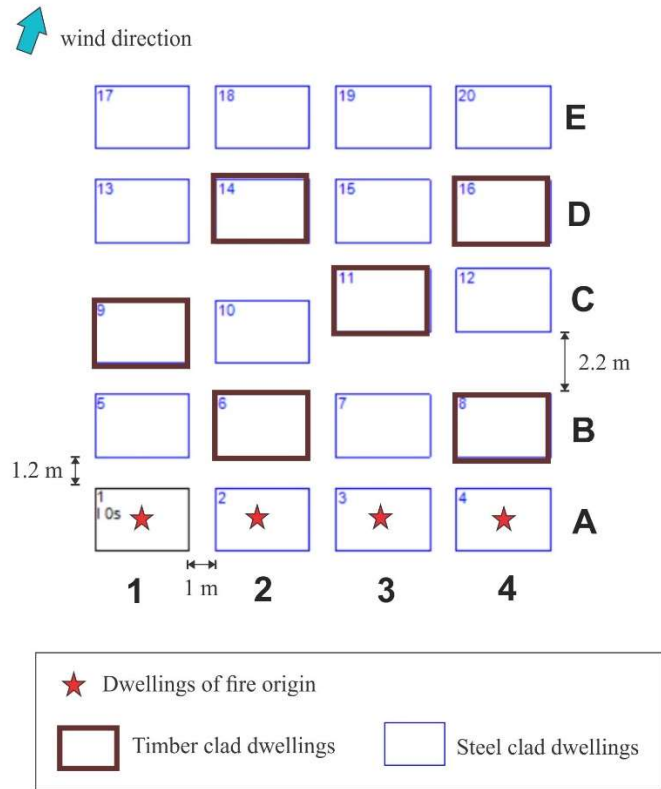
245

246

247

248

At the end of 2018, Stellenbosch University and the University of Edinburgh conducted the world's largest informal settlement dwelling fire experiment to date in Worcester, South Africa [8]. The experiment consisted of 20 dwellings, with all dwellings having a floor area of 3.6 m × 2.4 m and a height of 2.2 m. All dwellings were lined with corrugated cardboard and had 6 timber cribs each, giving an approximate fuel load of 24 kg/m² per dwelling. Each crib consisted of 28 × 0.48 m × 0.48 m × 1 m timber pieces, stacked as 7 alternating layers of 4 lengths. The experimental setup along with the details of the 20 dwelling burn experiment needed for this paper is depicted in Figure 7. For more information about the 20 dwelling burn experiment the reader should refer to [8], with a video of the experiment presented at: <https://youtu.be/kkXr6ueakAU>. The fire was started simultaneously in dwellings A1-A4 and was left to spread from the left of Figure 7 to the right. "Timber" or "Sheeting" in the figure legend imply that the dwelling was clad with timber planks or corrugated steel sheeting, respectively. The wind blew at approximately 20 km/h (5.6 m/s) from a west-northwesterly direction depicted in Figure 7.



249

250

Figure 7. Layout of the 20 dwelling fire experiment [8].

251

252

253

254

255

256

257

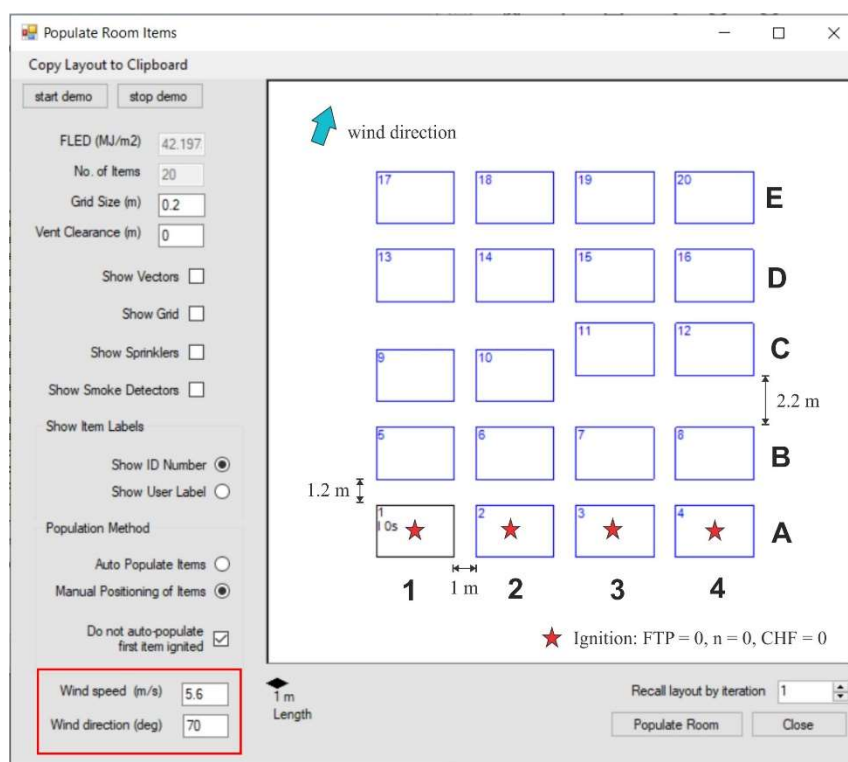
258

259

260

261

The geometric setup of the B-RISK 20 dwelling simulation is depicted in Figure 8. For dwellings 1-4 (i.e., A1-A4 in Figure 7), all ignition criteria (*FTP*, *n* and *CHF*) were set to 0 to ensure that the dwellings ignite simultaneously as soon as the simulation started. For the remaining dwellings, the ignition criteria of Cardboard 2 (i.e., the cardboard used for internal lining in the 20 dwelling experiment), as listed in Table 1, has been used. For the simulations that follow, it is postulated that, for timber clad dwellings, the cardboard lining ignites before the timber cladding (i.e. since the cardboard has lower CHF, FTP values and FTP index values compared to the timber, and since both the cardboard and timber are exposed to the same incident heat flux). Observations in the 3 timber clad dwelling experiment [9] with similar configurations as used here, highlighted this phenomena where the cardboard ignited, experienced rapid fire spread across its surface inside the dwelling, and was the primary cause of flashover.



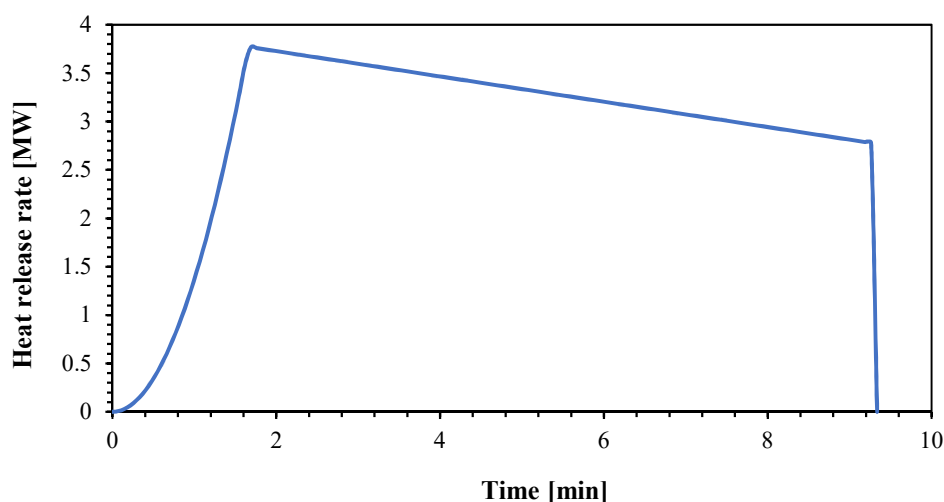
262

263 **Figure 8.** Annotated room (fully open to ‘outside’) setup in B-RISK, where ISDs A1-A4, B1-B4, C1-C4, D1-D4
 264 and E1-E4 are modelled as items. Wind direction used B-RISK setup is 70 degrees and wind speed as 5.6 m/s.

265 Using the crib model discussed by Babrauskas [27], it was determined that the crib mass loss
 266 rate in these dwellings were most likely fuel surface area-controlled. Using the heat of combustion as
 267 16.8 MJ/kg [8], and assuming the structures collapse approximately 7.1 minutes after the maximum
 268 heat release rate (HRR) is reached [28] (based on an averaged value from multiple experiments), the
 269 HRR curve depicted in Figure 9 is obtained. Although the dwellings clad with timber planks will
 270 have higher HRR (since the timber planks will contribute to the total fuel load and the total HRR),
 271 the initial growth period of timber clad dwellings are assumed to be unaffected by the timber planks
 272 (controlled by the cribs) and since the timber planks are thin (12 mm thick) it is assumed that it will
 273 burn away rapidly after the planks start burning [6,7]. Hence for simplicity, it was decided to assign
 274 the HRR curve depicted in Figure 9 to all dwellings for baseline simulation. However, to investigate
 275 the sensitivity of the HRR curve of the timber dwellings, three parametric simulations were run, as
 276 discussed below. The HRR values in the curve depicted in Figure 9 were increased by 20%, 50% and
 277 100% (i.e. the fuel load contribution of the timber planks have been used to increase the area under
 278 the HRR curve [7]), respectively. It was found that when the timber dwellings had HRR values 50%
 279 greater than the steel dwellings (Figure 9), the predicted spread rates are closer to the experimental
 280 spread rates, as depicted in Figure 10.

281 The maximum transient HRR of the timber used is around 200 kW/m², with a stable HRR of 100-
 282 150 kW/m², as determined by a cone calorimeter [23]. If this value is multiplied by the surface area of
 283 the timber cladding the maximum HRR increases by approximately 2.3-4.6 MW for each side of the
 284 wall. However, due to ventilation control inside an ISD, and air not being able to reach dwellings
 285 within the settlement due to combustion occurring in the surrounding dwellings, the full HRR of the
 286 combined fuel plus cladding will not be reached. If it is assumed that only the outside of an ISD

287 contributes to the increased HRR at an average of 100 kW/m² (lower bound used since not all of the
 288 surface area may burn at the same time and lack of free flow air between the ISDs within the
 289 settlement), this gives an increased HRR of 60%, although it is possible that an increase in HRR of
 290 100% would be possibleconceivable.
 291



292

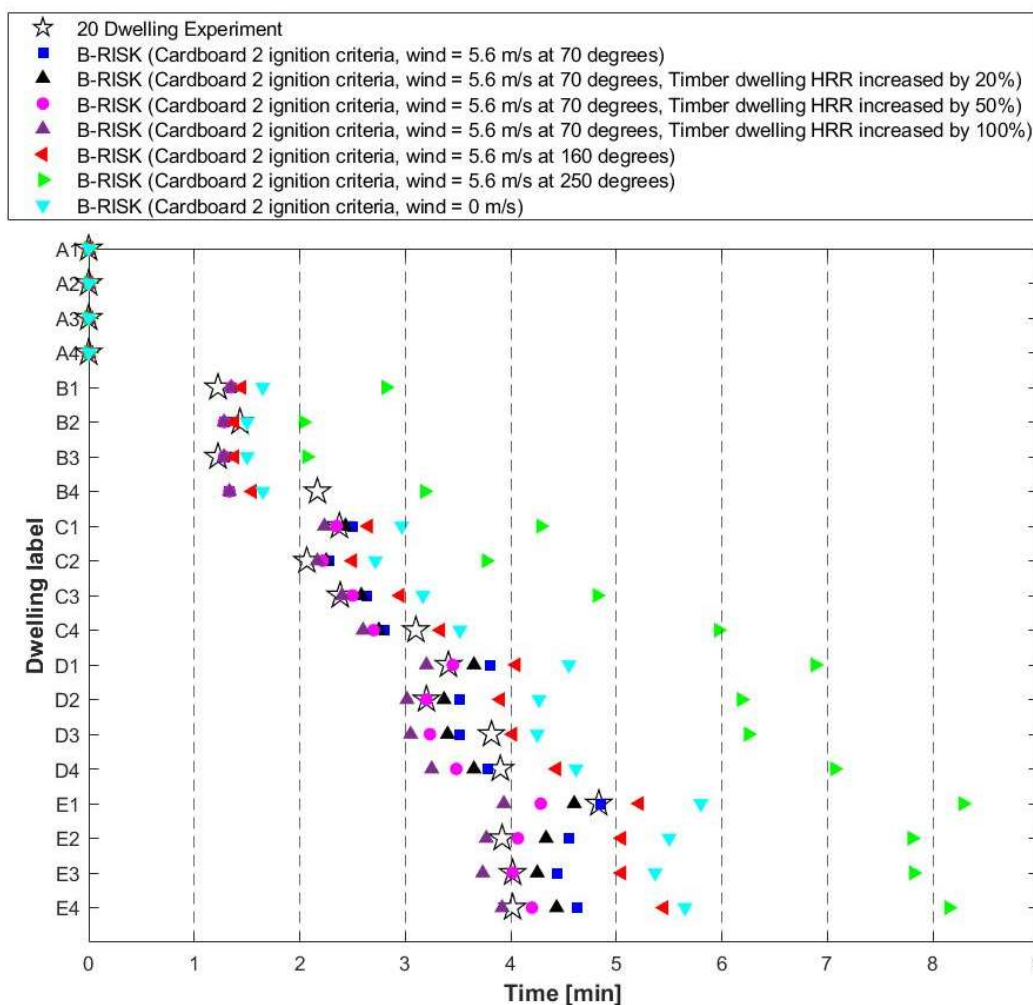
293 **Figure 9.** Baseline heat release rate curve for the dwellings used in the 20 dwelling experiment.

294 A soot yield of 0.015 g/g, CO₂ of 1.33 g/g and radiant loss fraction χ_R of 0.3 were taken from Table
 295 3-4.14 of the SFPE Handbook [20]. The heat of gasification (1.8 kJ/g) was selected from Table 3-4.7
 296 of the SFPE Handbook [20] to represent the overall average fuel load, based on similar representative
 297 materials. It should be noted that since this work only makes use of the radiation and ignition
 298 submodels, the exact values of the parameters specified above are not critical (i.e. they are not used
 299 in the submodels, except for the radiant loss fraction), but B-RISK requires values to be specified.
 300

301

301 3.2. Experimental versus numerical results

302 The results of the 20 dwelling experiment and B-RISK simulations are depicted in Figure 10. For
 303 the baseline simulation (Cardboard 2 ignition criteria, wind = 5.6 m/s at 70 degrees), where the wind
 304 conditions are the same as the experiment, B-RISK shows good correlation to the 20--dwelling
 305 experiment. The time-to-ignition of the dwellings in row A to D have negligible variation between
 306 the simulation and experiment, with only row E showing slightly slower times-to-ignition (30-40 s
 307 slower) compared to the experimental times. This could be as a result of the timber cladding
 308 contributing to the HRR not being accounted for in the baseline simulation, which is evident when
 309 considering the simulation where the items that represent the timber dwellings were assigned an
 310 increased HRR of 50%.



311

312

Figure 10. Experimental and simulation time-to-ignition results for different configurations

313

314

315

316

317

318

319

320

321

322

323

324

325

326

327

328

329

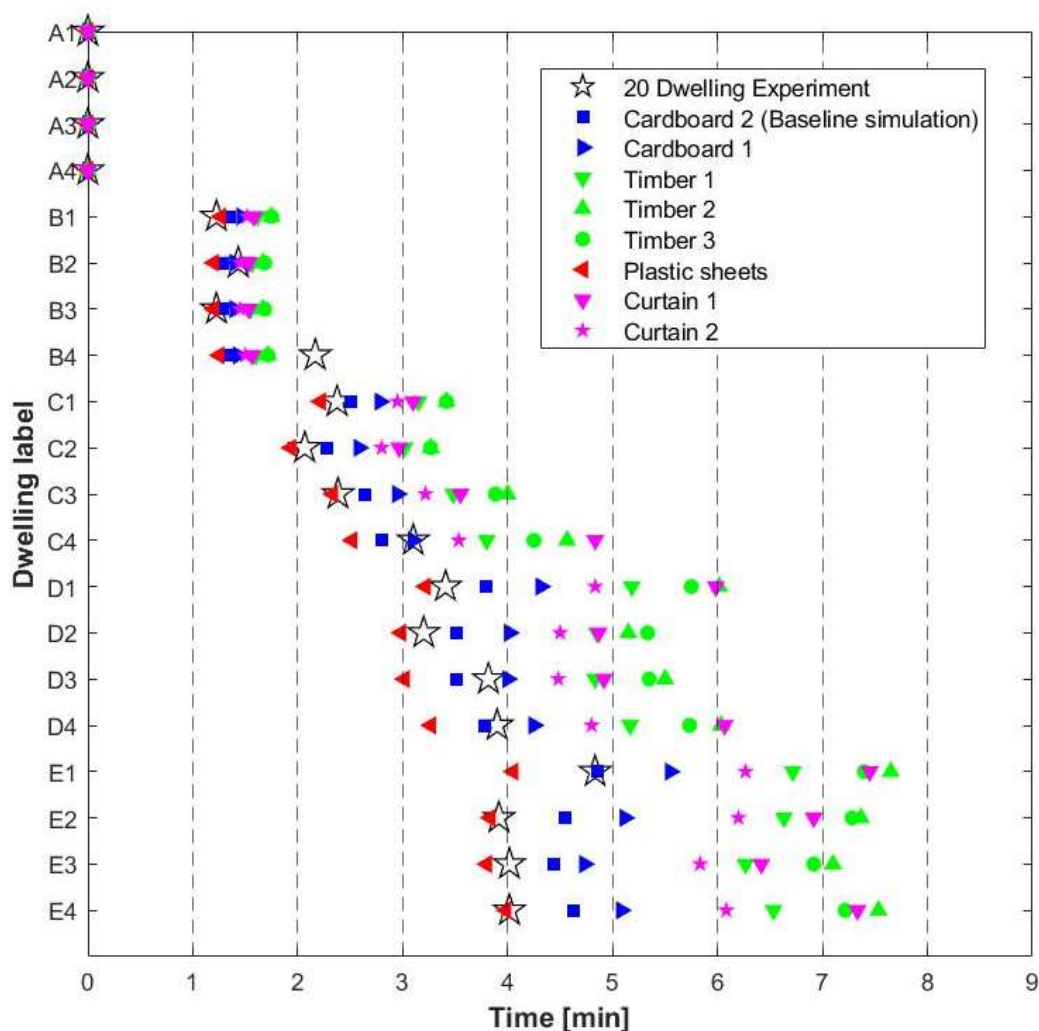
330

For interest, some variations of the baseline simulation (Cardboard 2 ignition criteria, wind = 5.6 m/s at 70 degrees) have been run to see the effect of the wind direction and wind speed, on the fire spread rates. Changing the wind direction by 90 degrees (Cardboard 2 ignition criteria, wind = 5.6 m/s at 180 degrees) does slightly decrease the time-to-ignition of the 20 dwellings compared to the baseline simulation (by under a minute for row E). For the simulation with no wind and wind in the opposite direction the time-to-ignition increased significantly (over 3 minutes for row E) compared to the baseline simulation, with the wind direction in the opposite direction having the greatest effect on increasing the ignition time as one would expect. Changing the wind direction by 180 degrees (i.e. in the opposite direction as fire spread) significantly reduces the likelihood of piloted ignition meaning that the assumption (i.e. the ignition criteria set is based on the assumption of piloted ignition) made in this case would not be correct. This means that the time-to-ignition values depicted in Figure 10 are likely over predicted (i.e. the time-to-ignition values would be much larger, or ignition might not have occurred, if auto-ignition values were assumed). For the no wind condition, it may initially be assumed that all dwellings in row B should ignite simultaneously due to them being equidistant to their corresponding neighbour in row A, however, it can be seen in Figure 10 that this is not the case. If the radiation sources (dwellings in row A) are considered, it is clear that dwellings B2 and B3 would receive radiation from three dwellings in row A whereas dwellings B1 and B4 on the edges of the experiment receive radiation from just ~~two~~ dwellings in row A.

331

332 3.3. Effect of ignition criteria

333 It is well known that ISDs are constructed from a variety of materials [29], and that no two
 334 dwellings are the same. The material used does not only vary from dwelling to dwelling, but also
 335 from settlement to settlement. As mentioned above, the original semi-probabilistic approach [10]
 336 demonstrated the predictive capabilities of the software against a real informal settlement fire, but
 337 found that the simulation overpredicted the spread rates. It was postulated that this was the result of
 338 a) human intervention in the early stages of the fire, and b) the use of only one set of ignition criteria
 339 (i.e., the ignition criteria of cardboard) for all dwellings. Hence, to investigate the effect of ignition
 340 criteria of the different combustibles listed in Table 1, a simulation for each set of ignition criteria ~~was~~
 341 has been run and compared to the original (Cardboard 2 ignition criteria, wind = 5.6 m/s at 70
 342 degrees) dwelling simulation, as depicted in Figure 11.



343

344 **Figure 11.** Effect of B-RISK simulation ignition criteria on time-to-ignition

345 Figure 11 clearly shows that the ignition criteria of the items play an important role in the spread
 346 rates predicted. In this case the time it took for all 20 dwellings to ignite can change by as much as 3.6
 347 min, i.e. 4 min for Plastic sheets to 7.6 min for Timber 2, which is a 90% increase in the time to ignition.
 348 Comparing the spread rates of Curtain 1 and Curtain 2, it seems that the CHF has a greater effect on

349 the fire spread rates compared to *FTP* and *n*. Since both the *FTP* value and the *FTP* index are higher
 350 for Curtain 2, one would expect the spread rate to be lower (slower spread), not higher (faster spread).
 351 Thus, since the spread rate of Curtain 2 is higher, it implies that the difference is as a result of the
 352 lower CHF (i.e. 34 kW/m² for Curtain 1 versus 23 kW/m² for Curtain 2).

353

354 3.4. Colour maps to investigate informal settlement layout configurations

355 In order to create a tool that can help government, local authorities and decision makers to
 356 simulate fires to quantify the magnitude of an incident to which they may need to respond, ~~or~~ to
 357 identify high risk settlements, or to identify high risk areas within a settlement, the output of such a
 358 tool needs to be understandable in a relatively non-technical manner. In the future, it would be
 359 advantageous to produce colour maps, showing the potential fire spread rates and patterns, of all
 360 informal settlements, e.g. in Cape Town for a prevailing wind direction. The colour maps would
 361 highlight the settlements most at risk to large conflagrations and would identify 'hot spots' within
 362 specific settlements. A visual depiction of fire spread rates would also help with evaluating the
 363 effectiveness of re-blocking and fire break strategies. Re-blocking refers to the collaborative
 364 reorganisation of home layouts in an area to provide a more efficient and structured community
 365 pattern, and is typically assisted by a municipal agency or other organisation (e.g. non-governmental
 366 organizations (NGO)).

367 Fire spread data can be graphically displayed in many ways as there are: instantaneous and
 368 averaged area spread rates [m²/h], instantaneous and averaged linear spread rates [m/h], heat release
 369 rate changes with time, and other such metrics. A simplified representation of the fire behaviour is
 370 presented below by plotting what is called a fire line linear progression rate [m/h], which is taken
 371 relative to the start of the simulation. Hence, the value is found by calculating the linear position of
 372 the fire line over the total time since time zero. The advantage of this metric is that it implicitly
 373 considers the time history of the fire behaviour. For example, if a fire has to cross a larger open
 374 distance which slows it down, all values on the far side of the open distance will be influenced by the
 375 delay. Other metrics, such as instantaneous spread rates, are useful in addition to this to see localised
 376 phenomena, but are not plotted in this paper due to space constraints.

377 As an illustration of the linear fire line progression rate, a colour map of the followings scenarios
 378 are depicted in Figures 12 – 15: a) the 20-dwelling experiment (Figure 12 a.) and the baseline
 379 simulation (Figure 12 b.); b) the baseline simulation, but where only dwelling A1 is ignited to see how
 380 it affects the spread rates and the spread pattern; c) the baseline simulation, where only dwelling A1
 381 is ignited, with a 3.5 m fire break between columns 2 and 3; and d) the baseline simulation, where
 382 only dwelling A1 is ignited, with a 4.5 m fire break between columns 2 and 3.. Note that for all cases
 383 the wind direction and wind speed were kept the same as the baseline case.

384 As stated above, the fire line progression rates [m/h] are calculated by dividing the equivalent
 385 radius of the burn scar at that particular time by the time-to-ignition (from the start of the simulation).
 386 For example:

$$387 \quad Sp_i = r_i / t_{ig_i} \quad (7)$$

388 where Sp_i is the spread rate [m/h] at index i , t_{ig_i} is the B-RISK time-to-ignition of dwelling i , and
 389 r_i is calculated as:

390

$$r_i = \sqrt{i \times L \times W \times (i/20)(C_f)/\pi} \tag{8}$$

391

where L is the length of the dwelling (3.6 m in this case), W is the width of the dwelling (2.4 m in this case)

392

and $(i/20)(C_f)$ is a 'correction' factor to account for the spacings between the dwellings (since

393

the area of these spacings are not explicitly calculated here), where 20 is the number of dwellings and

394

C_f is the total area (i.e. the area that encapsulate all the dwellings) divided by the sum of the area of

395

all the dwellings. This is done for all items and the calculated fire line progression rate of an item is

396

assigned to the four corners of the dwelling under consideration. The x and y axes of the colour maps

397

are the Cartesian coordinates of the domain (the room) in plan, where the bottom left corner is (0,0)

398

of the domain and it is the bottom left corner of dwelling A1 (Figure 8).

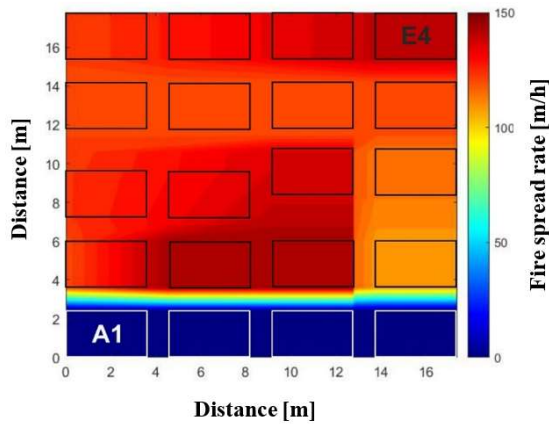


Figure 12 a. Colour map depicting the fire line progression rate relative to time zero, and pattern of the 20 dwelling experiment, where dwellings A1 to A4 are ignited.

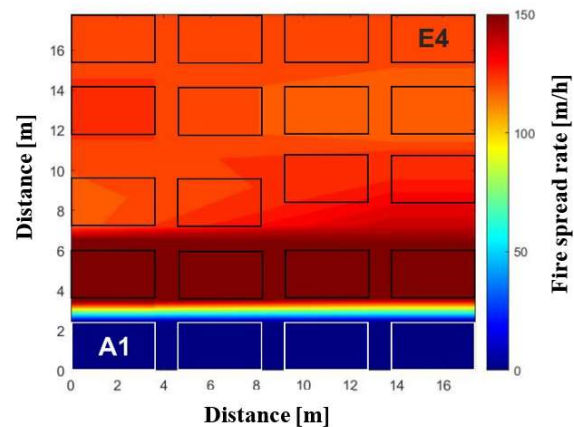
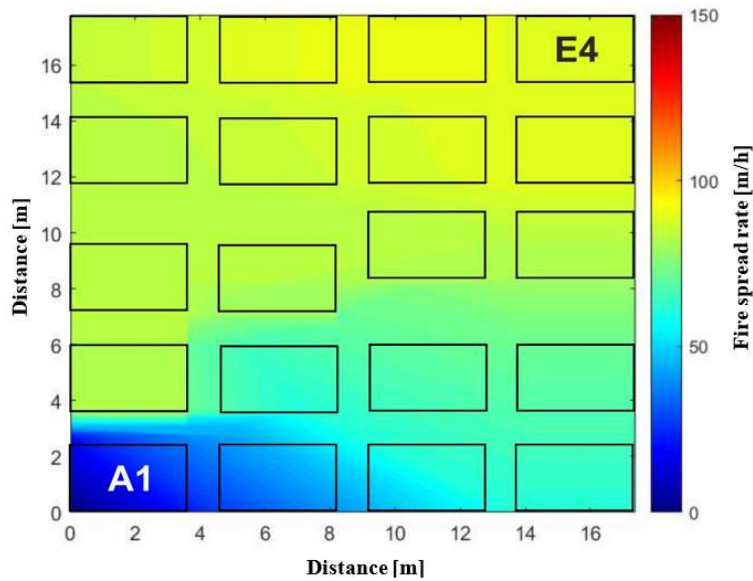


Figure 12 b. Colour map depicting the fire line progression rate relative to time zero, and pattern of the baseline simulations, where dwellings A1 to A4 are ignited.



399

400

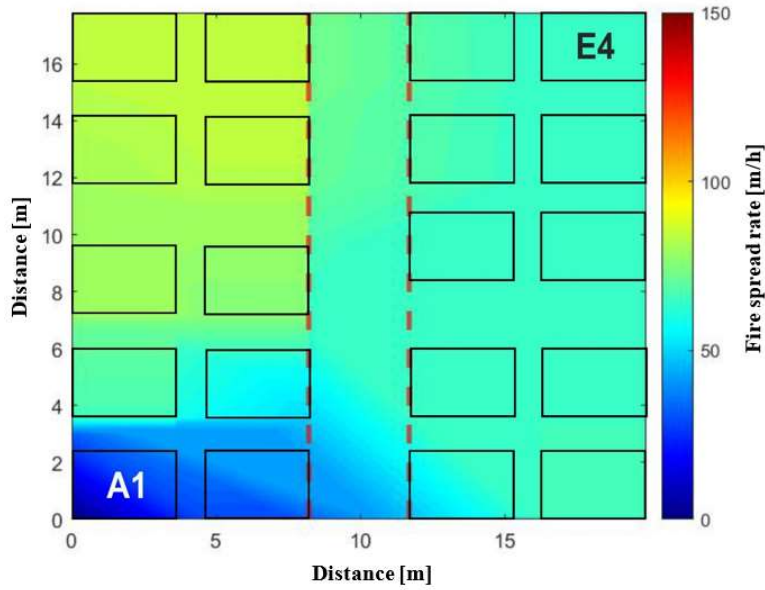
Figure 13. Colour map depicting the fire line progression rate relative to time zero, and pattern of the baseline

401

simulation, where only dwelling A1 is ignited

402

403

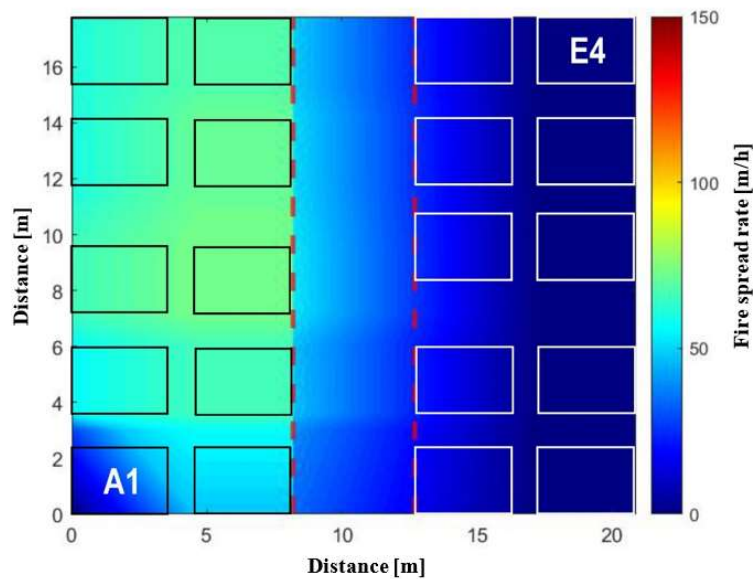


404

405

406

Figure 14. C Colour map depicting the fire line progression rate relative to time zero and pattern of the baseline simulation, where only dwelling A1 is ignited with the 3.5 m fire break marked by dotted red lines.



407

408

409

Figure 15. Colour map depicting the fire line progression rate relative to time zero and pattern of the baseline simulation, where only dwelling A1 is ignited with the 4.5 m fire break marked by dotted red lines.

410

411

412

413

414

415

416

417

418

Considering Figure 12 – Figure 15, the proposed colour map output ~~seems~~ appears to be producing realistic results. Comparing Figure 12 a) and b) to Figure 13, a decrease in maximum spread rate, of approximately 47% is observed. This is expected since igniting ~~four~~ dwellings simultaneously (Figure 12 a) and b)) would generate a significantly greater combined HRR initially than a single dwelling (Figure 13) which would ultimately lead to faster fire spread. Also, for the case where ~~four~~ dwellings are ignited simultaneously, there are more ISDs on fire in close proximity to others to ignite. Fire breaks are known to stop or reduce fire spread, and this is also reflected in the colour maps produced (Figure 14 and Figure 15). A number of studies have investigated the critical separation distance needed between ISDs for fire spread not to occur. Cicione *et al.* [9] found that for

419 'still' wind conditions, a distance of 3.8 m between ISDs is needed for fire spread not to occur. This
420 distance was calculated by fitting an exponential function of heat flux emitted versus distance from
421 dwelling to the experimental results. Based on this curve, it was found that at approximately 3.8 m
422 the heat flux emitted by a single dwelling would be less than the critical heat flux of cardboard. This
423 distance however neither accounts for wind effects nor for the effect of multiple dwellings burning
424 and emitting ~~heat-energy~~ simultaneously. Cicione *et al.* [7] used predictions from Fire Dynamics
425 Simulator to determine that, based on model uncertainties there is a probability of 6% (i.e. using the
426 method proposed in the "Calculating model uncertainty" section of the FDS validation guide [30])
427 that the heat flux (predicted by the FDS simulations) received at 3 m away from a single ISD would
428 exceed the assumed CHF of cardboard. Once again, the study did not consider wind, nor did it
429 consider the effect of multiple dwellings burning and emitting ~~heat-energy~~ at the same time. Wang
430 *et al.* [31] also found that for 'still' wind conditions, a distance of 3 m between ISDs is needed for fire
431 spread not to occur. Considering Figure 14, it can clearly be seen that, although a 3.5 m separation
432 (i.e., the fire break) did reduce the fire spread rate compared to the no fire break case as depicted in
433 Figure 14, the fire was still able to spread between columns 2 and 3 (Figure 7). However, it should be
434 noted that piloted ignition has been assumed in the ignition submodel, but with a 3.5 m separation
435 between dwellings it is less likely that flame impingement will occur. On the other hand, increasing
436 the fire break from 3.5 m to 4.5 m ~~we simulated clearly see that~~ fire spread ~~now-diddoes~~ not occur
437 and ~~that~~ the fire ~~was-is~~ contained to only one half of the mock settlement. Running the simulation for
438 different separation distances, the minimum distance at which fire spread did not occur was 4.2 m.
439 Thus, these B-RISK simulations indicate that when the effects of wind and multiple dwellings
440 burning at the same time are accounted for, a separation distance of 3.5 m is not sufficient, but rather
441 a distance of at least 4.2 m is needed. It is however acknowledged that such a large separation distance
442 is not always possible in reality as a result of socio-economic issues and insufficient spatial planning.
443 Additionally, it should be noted that for higher wind speeds and different wind directions this critical
444 distance might change, however these factors could be captured by using simulation tools such as B-
445 RISK. Also, branding was not accounted for in this work, which could also significantly affect the
446 critical separation distance.

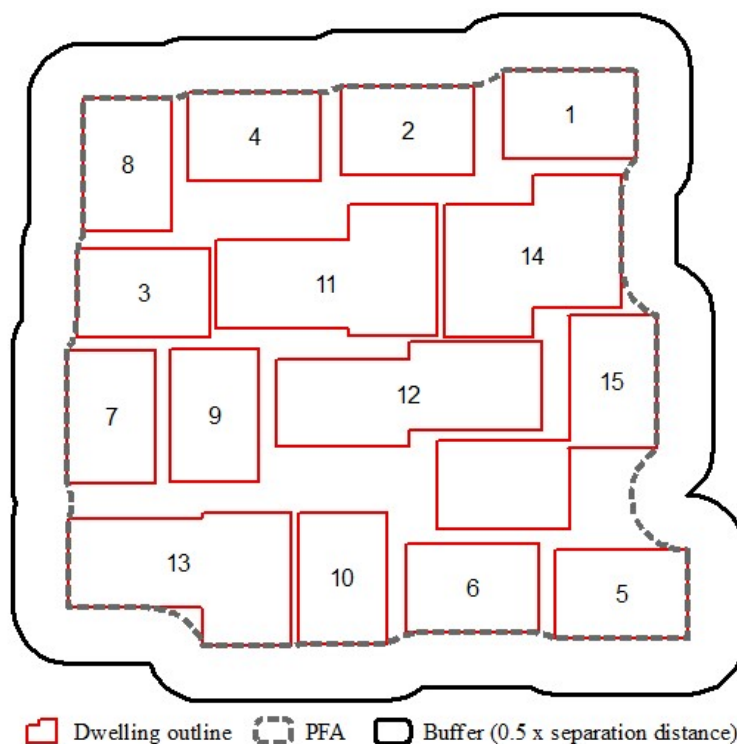
447 The colour maps illustrate the first step towards producing risk maps for informal settlements
448 using B-RISK, which may be a useful tool for fire brigades and local municipalities. In an ideal version
449 of the software, the user would be able to import settlement geometry from a GIS file and run limitless
450 iterations, by (1) randomly choosing a dwelling to ignite, (2) randomly allocating ignition criteria for
451 each dwelling and (3) randomly assigning a HRR for each dwelling. The software would be able to
452 consider varying wind conditions and produce an averaged colour map. This would highlight
453 dwellings most at risk within a certain settlement either regardless of wind conditions or for
454 particular wind conditions. In this paper a number of simplifications have been made to calculate the
455 fire line progression rates used to generate the colour maps and should not be considered as 'real'
456 values. The purpose of these colour maps is to illustrate the possibilities of this work and to show the
457 potential benefits of expanding B-RISK capabilities to produce these colour maps.

458

459 4. Spatial metrics

460 Gibson *et al.* [11] and Gibson *et al.* [32] first investigated various spatial metrics with respect to
461 fire spread in informal settlements in Cape Town. Gibson *et al.* [32] report that, when using dwelling
462 footprints mapped from LiDAR data, density (defined as the total dwelling footprint as a percentage
463 of the settlement area) and edge density (defined by the sum of all dwellings' perimeters per hectare)
464 can be used to identify settlements at risk of fire spread. Gibson *et al.* [11] found that the settlement
465 average of the distance to a dwelling's first nearest neighbour, together with the standard deviation
466 can be used to identify settlements at risk of fire spread. A relationship to edge density was also
467 found. That study also used the distance to a dwelling's first and third nearest neighbour to identify
468 particular dwellings within a settlement most at risk of fire spread. It should be noted that in this
469 work a single dwelling is defined as a structure with a single roof, or where roofs touch each other
470 and therefore individual structures cannot reliably be distinguished. However, in many instances a
471 dwelling may be subdivided internally and have multiple families or rooms within it, but this is very
472 difficult to identify from the aerial photography from which the roofs were digitised [33].

473 In this paper, average distance [m] from a dwelling to its first through to fifth nearest neighbour
474 (NN1...NN5), edge density [m/ha], and density [%] are calculated for each new layout generated in
475 B-RISK. Figure 16 illustrates an example of a settlement layout with Table 2 demonstrating how the
476 spatial metrics are calculated. It should be noted that dwellings which adjoin are, for the purposes of
477 the spatial metrics calculation, assumed to be a single dwelling. Some spatial metrics such as density,
478 require a confining area for which the spatial metric should be calculated. Gibson *et al.* [11] proposed
479 a method where dwellings which fall within the potential fire spread separation distance of each
480 other, are included in the same 'potential fire area' (PFA). In this paper, the critical separation distance
481 determined through the modelling has been used. Dwellings are firstly buffered (see Figure 16) using
482 half the critical separation distance. Buffering refers to a reclassification/adjusting of the area under
483 investigation, based on offsetting the perimeter by a specific amount. Firstly, any dwelling within
484 the separation distance of each other, are joined in the same buffered area, i.e. a polygon outlining
485 the area considered. Secondly, the resulting polygon is then buffered back by half the separation
486 distance so that the border of the PFA aligns with outermost walls of the outermost dwellings, and
487 the outermost dwellings are connected by the outline of the buffer. This technique is useful tool for
488 creating a polygon around a number of individual homes that could burn in a single fire, and ignoring
489 adjacent homes to which the fire would not spread.



490

491 **Figure 16.** Example settlement demonstrating the construction of the PFA. Dwellings are buffered outwards by
 492 $0.5 \times$ the separation distance. The resulting polygon is then buffered back by the same distance to obtain the
 493 PFA aligning with the walls of the outermost dwellings. Numbers in each dwelling correspond to the ID in
 494 Table 2.

495 Density and close proximity of dwellings has been stated as a cause for rapid fire spread in
 496 informal settlements [25]. By analysing the density of dwellings together with the average distance
 497 to nearest neighbours (NN1...NN5), a more nuanced understanding of the settlement layout and its
 498 impact on fire spread can be obtained. For example, if a settlement has a low average distance to NN1
 499 but high average distance to NN2...NN5, it implies that fire will more likely spread from the ignited
 500 dwelling to NN1 in a stepwise manner, and the fire is more likely to spread in only single directions
 501 (i.e. since the distance to NN2...NN5 might be far enough for spread to those neighbours not to
 502 occur). However, if a low average distance to NN1...NN5 is discovered, the spread will be radial as
 503 an ignited dwelling will be able to spread to more neighbours more easily. Through analysing these
 504 spatial metrics together with fire spread rates, it will become apparent which of these metrics are the
 505 most influential. For example, it may be that the density metric captures the information contained
 506 in the average distance to NN1...NN5 in which case for future studies, distance to NN will not be
 507 required, streamlining the processing.

508 The importance of edge density has been raised here since dwellings are ignited and spread from
 509 their edges. The logic therefore follows that settlements with a high edge density (i.e. many longer,
 510 thinner homes) offer more opportunities for fire to spread than settlements with low edge density.
 511 The two previous papers by Gibson *et al.* which investigated this revealed some correlation and
 512 therefore the role of this spatial metric is further explored here to determine its importance.

513

514 **Table 2.** Spatial metrics calculated for the settlement shown in Figure 16.

ID	Perimeter (m)	Area (m ²)	NN1:ID <i>distance</i> (m)	NN2:ID <i>distance</i> (m)	NN3:ID <i>distance</i> (m)	NN4:ID <i>distance</i> (m)	NN5:ID <i>distance</i> (m)	
1	12	8.64	14 0.45	2 0.80	11 2.16	15 4.27	4 4.97	
2	12	8.64	4 0.60	1 0.80	11 0.80	14 0.82	3 4.10	
3	12	8.64	11 0.19	9 0.35	7 0.37	8 0.47	4 1.83	
4	12	8.64	8 0.42	2 0.57	11 1.00	3 1.83	14 3.44	
5	12	8.64	6 0.45	15 0.58	12 3.27	10 4.59	14 5.81	
6	12	8.64	15 0.40	5 0.44	10 0.55	12 2.62	13 3.15	
7	12	8.64	3 0.37	9 0.40	13 0.98	11 1.76	8 3.24	
8	12	8.64	4 0.42	3 0.47	11 1.23	9 3.22	7 3.24	
9	12	8.64	3 0.35	7 0.40	12 0.49	11 0.58	12 0.83	
10	12	8.64	13 0.20	6 0.55	9 1.34	15 1.37	12 1.77	
11	19.2	17.28	12 0.15	14 0.19	3 0.19	9 0.58	2 0.80	
12	20.1	17.28	14 0.13	11 0.15	15 0.27	9 0.49	10 1.77	
13	19.2	17.28	10 0.20	9 0.83	7 0.98	12 1.78	6 3.15	
14	18.4	17.28	12 0.13	11 0.19	15 0.22	1 0.49	2 0.82	
15	23.6	17.28	14 0.22	12 0.27	6 0.40	5 0.58	10 1.37	
Sum	220.5	172.8						
Average			0.31	0.47	0.95	1.69	2.69	
PFA		231.26						
Density (%)	= Sum Area / PFA × 100 = 172.8 / 231.26 × 100 = 74.7			Edge density (m/ha) = Sum Perimeter / PFA × 10 000 = 220.5 / 231.26 × 10 000 = 9535				

516 5. Identifying spatial metrics that are indicative of higher fire spread risk

517 To determine which spatial metrics are the most influential for informal settlement fire spread,
518 the radiation and ignition submodels of B-RISK are used (discussed in Section 3) to predict fire spread
519 rates for a variety of randomly populated ‘informal settlement’ configurations. From these, the
520 average spread rates (i.e. depending on which dwelling ignited first in the populated scenario) ~~are~~
521 have been obtained and the spatial metrics of the corresponding settlement scenario are calculated.
522 In this case, 25 different settlement configurations, consisting of 20 dwellings each (which were the
523 same as the baseline dwellings used in Section 3), were randomly populated (i.e. the location of the
524 dwellings were randomly populated). Each settlement scenario thus had a different dwelling layout
525 configuration resulting in different spatial metrics values, an example of which can be seen in Figure
526 16 and Table 2.

527 For each scenario, the average time to ignite all 20 dwellings ~~was~~ has been determined, with each
528 dwelling in the settlement configuration given a chance to ignite first. This resulted in 20 different
529 times to ignite the whole layout for the same scenario (a total of 500 calculated fire spread rates) from
530 which the average time-to-ignition and the average spread rates ~~were~~ are determined. To ensure a
531 variety of settlement densities ~~was~~ have been captured, 10 scenarios ~~had~~ have a domain (i.e. the room
532 floor area in B-RISK) of 17.5×17.5 m to simulate very dense settlements (70-79% density), 10 scenarios
533 ~~had~~ have a domain of 18.3 × 18.8 m (same as the 20-dwelling experiment) to simulate slightly less
534 dense settlements (56-67 %), and 5 scenarios ~~had~~ have a domain of 20.5 × 20.5 m to simulate less dense
535 settlements (57-61%). Density refers to the percentage% of area covered by dwellings and a
536 comparison to densities found in reality is considered when the results are discussed below.
537 Although burned areas of large fires have been found to have densities at or exceeding the density
538 given in the “very dense settlement” scenario [11], less dense settlements ~~were~~ have been simulated
539 to capture a wider variety of spatial metrics beyond just density. It should be noted here that the
540 dwelling locations for scenarios randomly populated in B-RISK are not automatically captured in an
541 output file, nor is the time-to-ignition. Hence, for the 500 simulations done in this work, all B-RISK
542 data ~~was~~ has been captured manually, as well as all spatial metric data, and thus only 25 settlement
543 scenarios ~~were~~ have been simulated. The fire spread rates for the 25 scenarios ranged from 2090 –
544 2958 m²/h. For future use, it would be advantageous to automate the process so that more simulations
545 can be carried out.

546 Based on the analyses conducted, an interesting question arises – can a simplified analytical
547 equation be developed to approximate fire spread based on measurable settlement metrics? Although
548 it is not possible to include factors discussed in the introduction (e.g. branding, suppression, fuels
549 between homes, etc.), predictions still provide a useful benchmark and tool for comparing and
550 quantifying risk. In ArcGIS 10.5, the dwellings for each scenario ~~were~~ have been digitised, the
551 potential fire spread area (PFA) for each scenario was created and the spatial metrics for each PFA
552 ~~were~~ are calculated. These spatial metrics, together with the B-RISK average fire spread rates ~~were~~
553 have been used to derive a linear equation (derived from the correlation between the dependent and
554 independent variables) to predict the average fire spread rate of an informal settlement using only
555 spatial metrics:

$$556 S_p(x_1, x_2, \dots, x_n) = ax_1 + bx_2 + \dots + zx_n + C \quad (9)$$

557

558 where S_p (the dependent variable) is the predicted potential average fire spread rate as a function of
 559 the settlement's spatial metrics [m^2/h] and x_1 to x_n (the independent variables, as defined below)
 560 are the spatial metrics. It should be noted that in the development of the equation, only spatial metrics
 561 from the simulated scenarios are used and these do not represent the full range of scenarios (and thus
 562 spatial metrics) that are found in reality. Thus, the application of the developed equations to PFAs
 563 with spatial metrics exceeding the range covered in the B-RISK scenarios are considered less reliable
 564 as this will be an extrapolation of the equation. The spatial metrics considered were density, edge
 565 density, average distance to NN1...NN5 as well as the additive metrics of NN1 and subsequent NNs
 566 e.g. NN1+NN2, NN1+NN3 and so on. The additive metrics ~~were~~have been considered due to the
 567 hypothesis by Gibson *et al.* [11] that consideration of NN1 and NN3 together better describes
 568 clustering in a settlement and therefore has an influence on fire spread. In order to obtain the
 569 coefficients of each independent variable in Equation 9, the least square method ~~was~~has been used
 570 and it is given by [34]:

$$571 \hat{\beta} = (X^T X)^{-1} X^T \hat{y} \quad (10)$$

572 where the matrix X contains the spatial metrics of interest (the parameters) for each scenario and the
 573 vector \hat{y} contain the actual spread rates predicted by B-RISK for each scenario. Using the Akaike
 574 Information Criterion (AIC) [34] the parameters that do not affect the fire spread rates ~~were~~are
 575 removed from Equation 9, where it ~~was~~is found that the density and the NN1+NN3 value gave the
 576 smallest AIC value (including any other spatial metrics made the AIC value higher). Hence, the final
 577 equation to determine potential fire spread rates for informal settlements is as follows:
 578

$$579 S_p = 20.5D - 278.1(NN_{1+3}) + 1742.3 \quad (11)$$

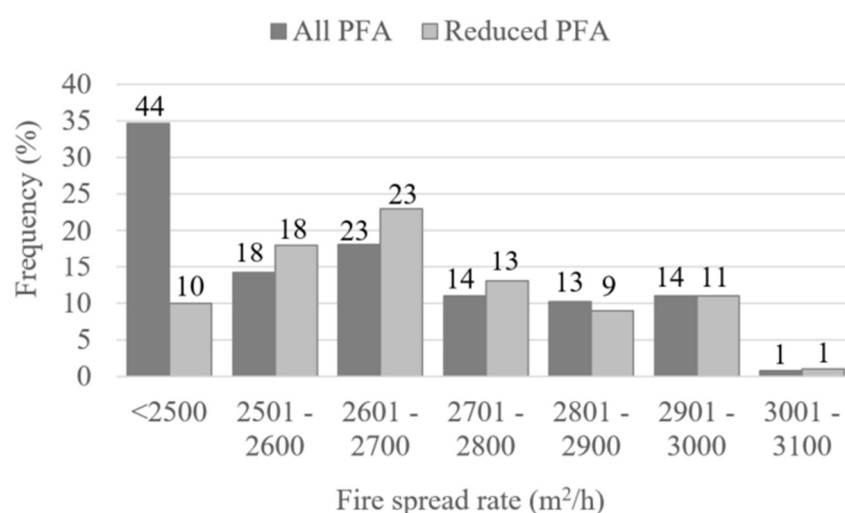
580 where D is the settlement density [%] and NN_{1+3} is the distance from the average distance to the
 581 first nearest neighbour plus the average distance to the third nearest neighbour [m].
 582

583 Informal settlement dwelling footprints are available for all informal settlements in Cape Town [33]
 584 and using this dataset the following procedure has been applied:

- 585 1. PFA's were created;
- 586 2. due to the large number of informal settlements in Cape Town, only PFA's larger than 1 ha
 587 were selected for subsequent analysis;
- 588 3. density and NN_{1+3} ~~was~~have been calculated for each PFA;
- 589 4. descriptive statistics of spatial metrics were calculated for both B-RISK scenarios and the
 590 PFAs; and
- 591 5. Equation 11 ~~was~~has been applied to arrive at a fire spread rate for each PFA.

592 This method ~~resulted~~resulted in a total of 127 PFAs larger than 1 ha for the City of Cape Town. The
 593 descriptive statistics ~~revealed~~revealed that the B-RISK scenarios capture a slightly different range of spatial
 594 metrics than is seen in PFAs with the B-RISK range in spatial metrics calculated as density: 56.4 –
 595 78.6%; and NN_{1+3} : 1.13 – 2.70 m compared with PFAs: density: 65.7 - 80.9%; and NN_{1+3} : 0.21 – 3.78 m.
 596 Of the 127 PFAs, 119 and 93 had densities and NN_{1+3} values which ~~fell~~fall within the B-RISK scenario
 597

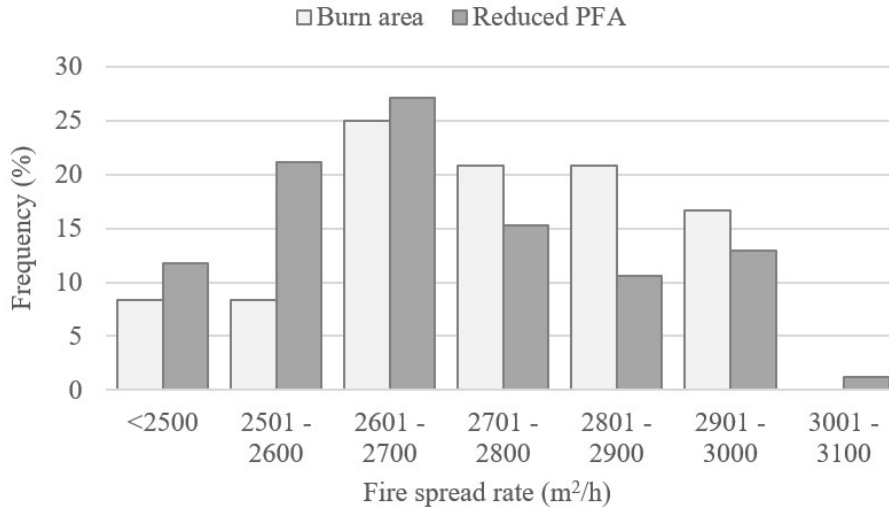
599 range respectively. 85 (67%) of PFAs ~~fell-fall~~ within the range of both spatial metrics used in the B-
 600 RISK scenarios. The densities which ~~fell-fall~~ outside of the B-RISK range, all exceeded the range used
 601 in B-RISK which ~~will-is~~ also ~~be-why~~, for these values, NN_{1+3} does not exceed the range used in the B-
 602 RISK scenario as these represent PFAs where the dwellings are in very close proximity to each other.
 603 Thus, the NN_{1+3} spatial metrics place a greater role in excluding PFAs from analysis than density. It
 604 can be seen in Figure 17 that where the spatial metrics of PFA overlapped with those of the B-RISK
 605 scenarios (shown as Reduced PFAs in the figure), the fire spread rate ~~was-is~~ highest. This implies that
 606 Equation 11 predicts high spread rates (greater than 2500 m²/h) more reliably than low spread rates
 607 across all PFAs since the equation was developed using scenarios which predict a higher spread rate
 608 and those PFAs which likely (but this is yet to be proven) have a lower spread rate were not used in
 609 the development of the equation. Note that fire spread rates less than 2500 m²/h are not displayed as
 610 there is no data in this range for Reduced PFAs.



611

612 **Figure 17.** Histogram showing predicted fire spread rates for all PFAs greater than 1 ha and also a reduced
 613 subset of PFAs where the spatial metrics of the PFA correspond with the spatial metrics used to develop the
 614 equation, shown as Reduced PFA on the graph. The count is displayed above each bar.

615 To consider if PFAs with high fire spread rates are in fact affected by large fires in reality, fire
 616 spread rates ~~were-are~~ obtained for burn areas which were previously mapped from satellite imagery
 617 [35]. These burn areas ~~were-are~~ assigned fire spread rates by spatially overlaying the Reduced PFAs
 618 with the burn areas and assigning the fire spread rate from the PFA to the overlapping burn area.
 619 Figure 18 reveals that the burn areas are more likely to be found in PFAs with higher fire spread rates
 620 implying that the fire spread rate equation is correct to some degree but since fire spread rates are
 621 not known for the mapped fires, this can be considered a qualitative rather than quantitative
 622 agreement.



623

624

625

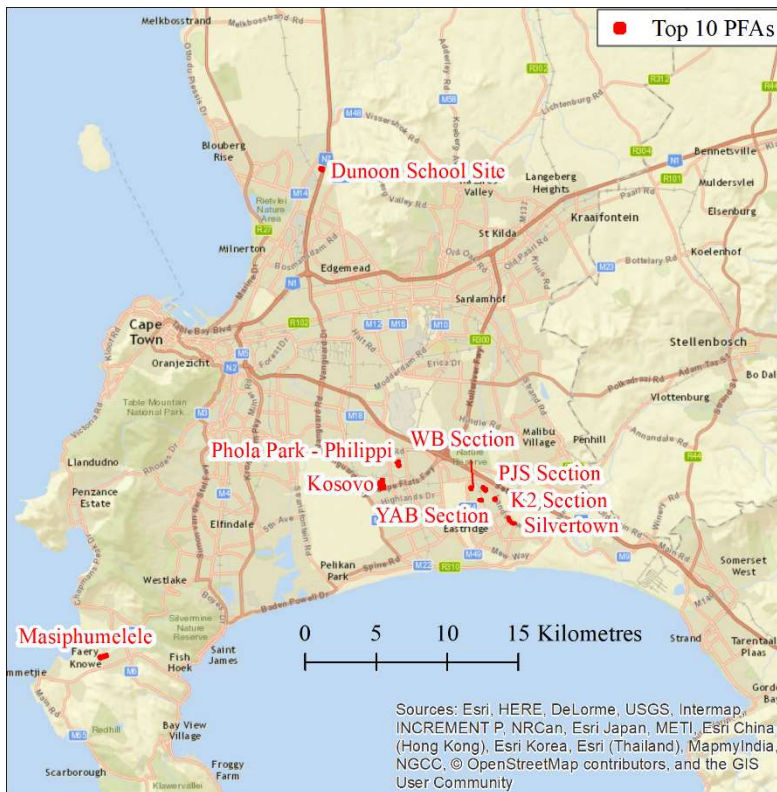
Figure 18. Histogram showing predicted fire spread rates for Reduced PFAs and burn areas mapped from satellite images.

626

627

628

The PFAs with the top ten (out of 127 PFAs) fire spread rates across all informal settlements within the City of Cape Town are given in Table 3 and the location of the PFAs is shown in Figure 19.



629

630

631

Figure 19. Location of the top 10 PFAs greater than 1 ha which have highest fire spread rate. (North is at the top of the images)

632

633

634

635

It can be noted that the top 10 PFAs are at or exceed the uppermost fire spread limit calculated in B-RISK (2958 m²/h) and two of the PFAs in the top 10 (Silvertown and PJS Section) slightly exceed the density used in the development of Equation 11 however due to their slightly larger NN₁₊₃ values, these PFAs do not have the highest fire spread rate. The results should therefore be treated as being

636 indicative of settlements at risk of fire spread rather than the fire spread rate be considered reliable –
 637 not least because the area covered by the top 10 PFAs far exceeds the area covered by 20 dwellings
 638 which were used in the development of the equation.

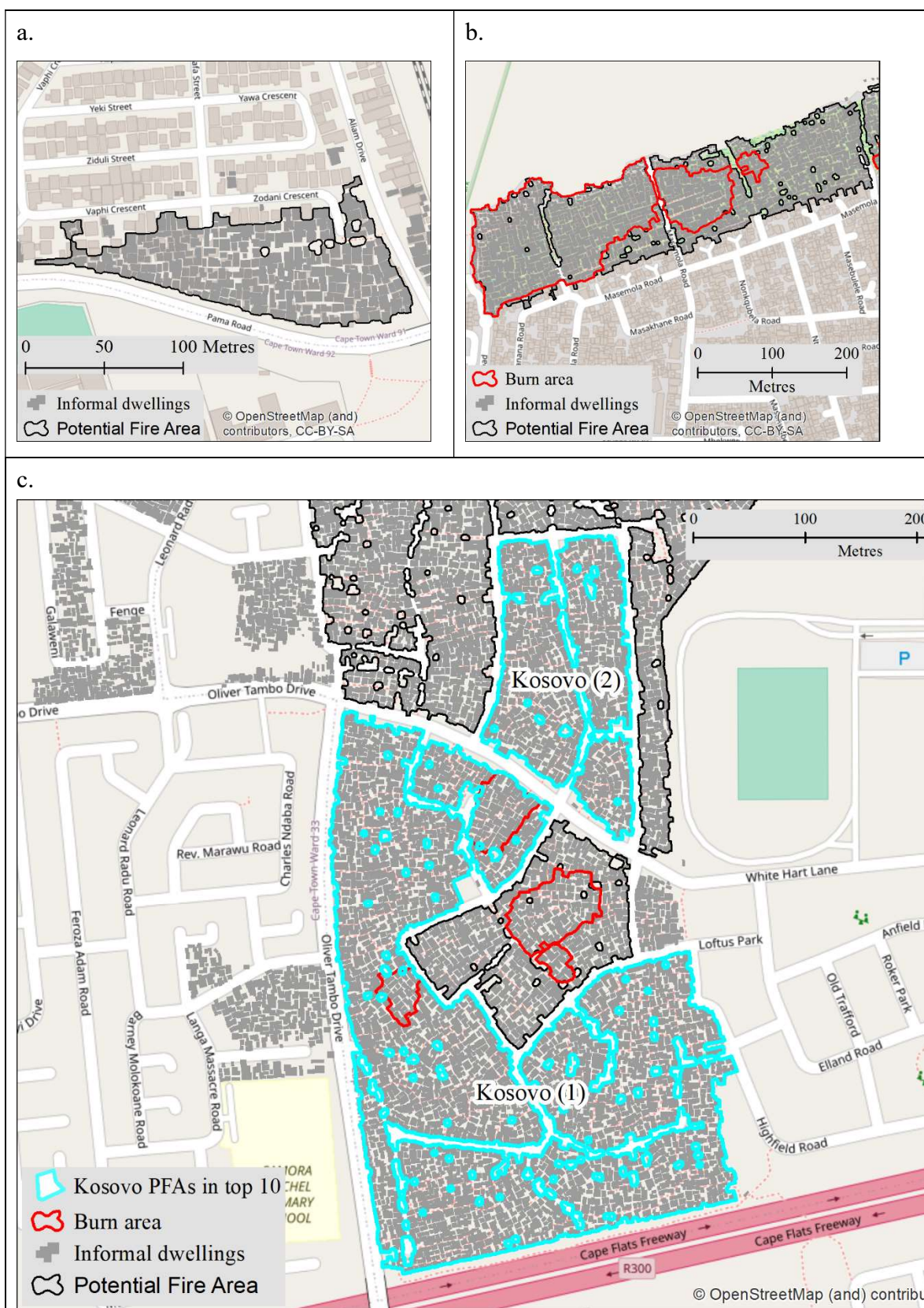
639 **Table 3.** PFAs with highest fire spread rates of the 127 PFAs studied in Cape Town, with corresponding spatial
 640 metrics

Settlement containing PFA	Area (m ²)	Density (%)	NN ₁₊₃ (m)	Fire spread rate predicted by Equation 11 (m ² /h)
YAB Section	10 143	77.9	1.21	3 002
K2 Section	12 156	76.6	1.27	2 960
Dunoon School Site	25 264	77.1	1.31	2 957
WB Section	12 527	75.1	1.21	2 942
Kosovo (1)	90 243	75.6	1.28	2 935
Silvertown	28 124	79.7	1.6	2 928
PJS Section	33 884	80.9	1.7	2 927
Phola Park - Philippi	28 344	75.8	1.3	2 926
Masiphumelele	60 411	77.2	1.4	2 923
Kosovo (2)	23 663	77.3	1.5	2 920

641
 642 It should be noted that even informal settlements with a 'low' calculated spread rate are likely still at
 643 a higher risk for large conflagrations compared to most formal neighbours, because of the inherent
 644 nature of these areas (i.e. dwellings are built extremely close to each other and built from highly
 645 combustible materials).

646 The size and shape of the selected top 10 PFAs are shown in Figure 20. YAB Section (Figure 20a),
 647 although the PFA with the highest fire spread rate, is the smallest of the top 10 PFAs with an area of
 648 just over 1 ha. Masiphumelele and Kosovo are the largest PFAs in the top 10 and the occurrence of
 649 fires in these settlements is documented [35] and displayed in Figure 20 b. and c. respectively. This
 650 implies that the size of the PFA should be considered together with the calculated fire spread rates
 651 when assessing the particular risk of a settlement. Since the B-RISK scenarios contained only 20
 652 dwellings, and radial fire spread [m²/h] is assumed, as the fire grows in a larger settlement, the fire
 653 spread rate will increase. Furthermore, the shape of a settlement will play a role too, since as radial
 654 fire spread is assumed, once the fire front reaches the boundary of a settlement, the fire spread rate
 655 will change from 'radial' to linear along the length of the settlement's boundary. In a settlement which
 656 has a high perimeter to area ratio, the fire will reach an edge beyond which the fire can no longer
 657 grow [36] and at that point, fire spread rate will become linear. The current modelling does not
 658 consider this.

659



660 **Figure 20.** Selected PFAs in the top 10. A. PFA with highest fire spread rate – YAB Section, b. Masiphumelele
 661 demonstrating fire occurrence within a PFA with high fire spread rate, c. the two PFAs in the top 10 located in
 662 Kosovo, a known informal settlement fire hot spot. Burn scars from known previous fires are indicated in red.

663 As expected, the equation produces fire spread rates that fall within realistic ranges where the
664 spatial metrics matched ~~the spatial metrics~~ those used in the equation's development, and since the
665 ranges used to develop the equation fell in the high fire spread rate side of the spectrum, the PFAs
666 highlighted as being at high risk, are likely to reflect reality. Also, fires mapped using satellite
667 imagery overlap with high fire spread rate PFAs but in the absence of a complete fire location and
668 size database, it is impossible to use this as anything other than a qualitative agreement. Fire
669 departments should thus be encouraged to collect accurate spatial location (GPS coordinates) when
670 they respond to fires as this will enable more accurate modelling which in turn will inform better fire
671 response management.

672 Although the fire spread rate equation shows promise, this equation is not yet well enough
673 refined to determine actual fire spread rates but rather indicates where settlements at higher risk of
674 fire spread are located. The assumption of radial fire spread in the modelling has been mentioned
675 and the shape of the settlements is likely to have an impact on the rate of fire spread with elongated
676 settlement representing less of a fire spread risk than more compact settlements. Additionally, it
677 should be considered to assign weight values to different settlement sizes, since large settlements
678 have the potential to become larger conflagrations. Finally, it is unknown how well the model
679 performed for settlements with spatial metrics outside the range of ~~the spatial metrics~~ those used to
680 develop Equation 11. Also Finally, B-RISK currently only allows for rectangular shaped dwellings
681 and the reality of what is found in informal settlements is different. Thus, at this stage, only
682 approximations of a narrow range of real-life dwellings have been included in the equation.

683 This research represents positive progress, however more work is needed before this method can
684 be used with confidence in real world scenarios. For future research it is recommended that: 1) a
685 larger variety of B-RISK simulations should be simulated to capture the full range of spatial metrics
686 in informal settlements of Cape Town; 2) explore the influence of settlement shape on the fire spread
687 rate; 3) increase the number of dwellings in the B-RISK simulations to capture nuances in the fire
688 spread risk when compared to the size of the settlement, and 4) improve the B-RISK capability to
689 automate the modelling process.

690 6. Future considerations

691 There have been a number of assumptions and simplifications made throughout this paper and
692 these have been highlighted throughout the paper. However, the hope is that the methodologies
693 developed in this paper would ultimately be of use for real settlements as a useful tool for fire fighters
694 and local municipalities. In order to achieve this, it is important that future work refines the
695 methodology by developing more robust methods for the assumptions made. As more data becomes
696 available from informal settlement dwelling experiments and from real fire incidents, the method
697 discussed in this work can be calibrated and updated to account for more variables. Before B-RISK
698 can be used in practice to simulate informal settlement fire spread rates and to determine settlements
699 at risk, the following are some considerations that need to be implemented or investigated in future
700 versions:

- 701 a) the radiation emitted from dwellings ~~should~~ could be calculated in a similar manner
702 proposed by Equation 5 in this work. Hence, each wall of the ISD will thus emit a different

- 703 incident heat flux based on the wall geometry (e.g. a wall with a window opening will radiate
704 more heat energy compared to a wall with no openings);
- 705 b) the ignition criteria selected should consider both wind direction and separation distances to
706 determine when the ignition criteria set should be auto- or piloted ignition;
- 707 c) the effect of changes in settlement (terrain) elevations ~~should be explicitly considered~~;
- 708 d) a functionality that accounts for irregular shape dwellings ~~should be added to the method~~;
- 709 e) the ability to include ISDs that are not orthogonal to each other in the domain;
- 710 f) the impact of convective cooling/heating ~~should be considered~~; and
- 711 g) the impact of combustible materials placed between ISDs ~~should be considered~~.

712 7. Conclusion

713 This paper investigates a semi-probabilistic and spatial metrics methodology for predicting and
714 mapping fire spread in informal settlements, considering a range of phenomena needed in the
715 development of such a tool. The effect of the ignition properties used in B-RISK on fire spread rates
716 between Informal Settlement Dwellings (ISDs) has been studied, based on the ignition criteria set
717 (FTP value, FTP index and critical heat flux) of a variety of combustibles typically found in informal
718 settlements. The current semi-probabilistic informal settlement fire spread model, proposed in
719 previous research by the authors, has been verified against a 20-dwelling full-scale ~~20~~ informal
720 dwelling settlement fire experiment, where the 20 dwelling B-RISK simulation shows good
721 correlation to the experiment. A limited parametric study of the 20 dwelling simulation has been
722 conducted, which highlights the effect of the ignition criteria set used. A number of simulations for a
723 real informal settlement fire, with relatively good data, have then been run with a variety of ignition
724 properties of typical cladding and lining materials used in informal settlements. The results show
725 that the ignition properties (hence the lining and cladding material used in ISDs) have a significant
726 effect on the rate of fire spread and can increase the fire spread rate by more than 90%.

727 The paper then takes the next step in developing a tool to identify settlements and areas in
728 settlements most at risk, by post-processing the B-RISK output data to generate colour maps of the
729 linear fire line progression rates and spread patterns. Colour maps of the 20 dwelling experiment and
730 parametric simulations have been created showing that for fire spread not to occur, a critical
731 separation distance of around 4.2 m between dwellings is necessary, based on these simulations and
732 the parameters used. This is larger than the previously proposed separation distance of 3.8 m, because
733 the wind effect and the influence of multiple dwellings burning at the same time were not previously
734 considered, but are accounted for in this work. A next step to this work would be to provide colour
735 maps (risk maps) for large informal settlements to determine which settlements are most at risk and
736 also to identify 'hot spots' within settlements.

737 The use of B-RISK to produce a fire spread rate equation using spatial metrics has been
738 demonstrated. A total of 500 simulations using 25 settlement scenarios were run in B-RISK and
739 average fire spread rates were calculated. Analysis of spatial metrics calculated for each scenario
740 reveal that settlement density and the average distance to the first nearest neighbour plus the distance
741 to the third nearest neighbour are the most influential spatial metric in predicting fire spread rate.

742 The fire spread rate equation has been applied to informal dwellings in Cape Town and 127 potential
743 fire spread areas (PFA) larger than 1 ha have been found. The PFAs with 10 highest fire spread rate
744 are presented and some of these PFAs are located in settlements known to be fire hot spots. Due to
745 the high level of uncertainty and variability associated with informal settlements, further research is
746 required to fine tune the equation to a more complete range of informal settlement layouts and to
747 account for the assumptions made in the modelling. Factors that are difficult to quantify in
748 settlements include the influence of suppression (from residents and firefighters), branding,
749 combustible material stored between dwellings, the presence of explosive items such as LPG
750 cylinders, and even fuel loads that move during events as people evacuate with their possessions.
751 However, the spread rates provide useful benchmarks and comparisons from which informed
752 decisions can be made, and with time the predictions will be refined. However, this work represents
753 a substantial step forward (a) in linking outputs from the B-RISK simulations to outputs for GIS to
754 help identify settlements at risk of fire spread, and (b) to create a risk management tool for
755 government and local authorities.

756

757 **Author Contributions:** Conceptualization, Antonio Cicione, Lesley Gibson, Colleen Wade and Michael
758 Spearpoint; Formal analysis, Antonio Cicione and Lesley Gibson; Funding acquisition, Richard Walls and David
759 Rush; Methodology, Antonio Cicione, Lesley Gibson, Colleen Wade and Michael Spearpoint; Software, Antonio
760 Cicione and Lesley Gibson; Visualization, Antonio Cicione and Lesley Gibson; Writing – original draft, Antonio
761 Cicione; Writing – review & editing, Antonio Cicione, Lesley Gibson, Colleen Wade, Michael Spearpoint,
762 Richard Walls and David Rush.

763 **Funding:** The authors would like to acknowledge the financial support of the Lloyd’s Register Foundation under
764 the “Fire Engineering Education for Africa” project (Grant GA 100093), the IRIS-Fire GCRF project from the UK
765 (Engineering and Physical Sciences Research Council (Grant no.: EP/P029582/1)), as well as the Royal Academy
766 of Engineering / Lloyd’s Register Foundation Engineering X programme under grant “A Fire Safe Africa” (Grant
767 ESMN1921\1\141).

768 **Acknowledgements:** The authors would also like to gratefully acknowledge BRANZ in New Zealand for their
769 support enabling modifications to the B-RISK model.

770 **Conflicts of Interest:** The authors hereby acknowledge the financial contribution of the following organisations
771 in the completion of this work: the Lloyd’s Register Foundation under the “Fire Engineering Education for
772 Africa” project (Grant GA 100093), the IRIS-Fire GCRF project from the UK (Engineering and Physical Sciences
773 Research Council (Grant no.: EP/P029582/1)), as well as the Royal Academy of Engineering / Lloyd’s Register
774 Foundation Engineering X programme under grant “A Fire Safe Africa” (Grant ESMN1921\1\141). None of
775 these organisations have vested interests in the work and no conflicts of interest exist in the publication of this
776 work.

777 References

- 778 1. FPASA, SA Fire Loss Statistics 2016, 2018.
- 779 2. World Health Organization, Burns, (2018).
- 780 3. A. News, Favela in flames: Aerial footage shows fire ripping through Brazilian slum, (2016).
781 <https://www.abc.net.au/news/2016-09-14/fire-sweeps-through-sao-paulo-favela/7843336>
782 (accessed April 9, 2020).
- 783 4. C. Kahanji, R.S. Walls, A. Cicione, Fire spread analysis for the 2017 Imizamo Yethu informal

- 784 settlement conflagration in South Africa, *Int. J. Disaster Risk Reduct.* (2019).
785 <https://doi.org/10.1016/j.ijdr.2019.101146>.
- 786 5. Y. Wang, M. Beshir, A. Cicone, R. Hadden, M. Krajcovic, D. Rush, A full-scale experimental
787 study on single dwelling burning behavior of informal settlement, *Fire Saf. J.* (2020).
- 788 6. A. Cicone, R.S. Walls, Towards a simplified fire dynamic simulator model to analyse fire
789 spread between multiple informal settlement dwellings based on full-scale experiments, *Fire*
790 *Mater.* (2020) 1–17. <https://doi.org/10.1002/fam.2814>.
- 791 7. A. Cicone, M. Beshir, R.S. Walls, D. Rush, Full-Scale Informal Settlement Dwelling Fire
792 Experiments and Development of Numerical Models, *Fire Technol. J.* (2019).
793 <https://doi.org/10.1007/s10694-019-00894-w>.
- 794 8. N. de Koker, R. Walls, A. Cicone, Z. Sander, S. Loffel, J. Claasen, S. Fourie, L. Croukamp, D.
795 Rush, 20 Dwelling Large-Scale Experiment of Fire Spread in Informal Settlements, *Fire*
796 *Technol.* (2020). <https://doi.org/DOI 10.1007/s10694-019-00945-2>.
- 797 9. A. Cicone, R.S. Walls, C. Kahanji, Experimental study of fire spread between multiple full
798 scale informal settlement dwellings, *Fire Saf. J.* 105 (2019) 19–27.
799 <https://doi.org/10.1016/j.firesaf.2019.02.001>.
- 800 10. A. Cicone, C. Wade, M. Spearpoint, L. Gibson, R.S. Walls, D. Rush, A preliminary
801 investigation to develop a semi-probabilistic model of informal settlement fire spread using
802 B-RISK, *Fire Saf. J.* (2020).
- 803 11. L. Gibson, A. Cicone, S. Stevens, R. Hadden, D. Rush, The influence of wind and the spatial
804 layout of dwellings on fire spread in informal settlements in Cape Town., (n.d.).
- 805 12. W.D. Walton, D.. Carpenter, C.. Wood, Zone Computer Fire Models for Enclosures, in: *SFPE*
806 *Handb. Fire Prot. Eng.*, 5th ed., Springer New York, 2016: pp. 1025–1033.
807 https://doi.org/10.1007/978-1-4939-2565-0_31.
- 808 13. C. Wade, G. Baker, K. Frank, R. Harrison, M. Spearpoint, B-RISK user guide and technical
809 manual, BRANZ Study Report SR364, Porirua, New Zealand, 2016.
- 810 14. S. Sazegara, M. Spearpoint, G. Baker, Benchmarking the Single Item Ignition Prediction
811 Capability of B-RISK Using Furniture Calorimeter and Room-Size Experiments, *Fire Technol.*
812 53 (2017) 1485–1508. <https://doi.org/10.1007/s10694-016-0642-y>.
- 813 15. M.Z.M. Tohir, The Capability of B-RISK Zone Modelling Software to Simulate BRE Multiple
814 Vehicle Fire Spread Test, in: *Asian Simul. Conf.*, 2017.
- 815 16. Building Research Establishment (BRE), Building Research Establishment: Fire Spread in Car
816 Parks, Eland House Bressenden Place London SW1E 5DU United Kingdom, BD2552 (2010),
817 2010.
- 818 17. G. Heskestad, Fire Plumes, Flame Height, and Air Entrainment, in: *SFPE Handb. Fire Prot.*
819 *Eng.*, 4th ed., Quincy, MA, USA, 2008: pp. 2–1 to 2–20.
- 820 18. Y. Oka, O. Sugawa, T. Imamura, Y. Matsubara, Effect Of Cross-Winds To Apparent Flame
821 Height And Tilt Angle From Several Kinds Of Fire Source, in: *Fire Saf. Sci.*, 2003: pp. 7:915-
822 926. <https://doi.org/10.3801/IAFSS.FSS.7-915>.
- 823 19. A. Cicone, R. Walls, Z. Sander, N. Flores Quiroz, V. Narayanan, S. Stevens, D. Rush, The effect
824 of separation distance between informal dwellings on fire spread rates based on experimental
825 data and analytical equations, *Fire Technol.* (2020).
- 826 20. A. Tewarson, Generation of Heat and Chemical Compounds in Fires, in: P.. DiNenno (Ed.),

- 827 SFPE Handb. Fire Prot. Eng., 3rd ed., 2016: pp. 277–324. [https://doi.org/10.1007/978-1-4939-](https://doi.org/10.1007/978-1-4939-2565-0_9)
828 2565-0_9.
- 829 21. T.J. Shields, G.W. Silcock, J.J. Murry, Evaluating ignition data using the flux time product, Fire
830 Mater. 18 (1994) 243–254. <https://doi.org/10.1002/fam.810180407>.
- 831 22. Y. Wang, C. Bertrand, M. Beshir, C. Kahanji, R. Walls, D. Rush, Developing an experimental
832 database of burning characteristics of combustible informal settlement dwelling materials,
833 Fire Saf. J. (2019). <https://doi.org/https://doi.org/10.1016/j.firesaf.2019.102938>.
- 834 23. Y. Wang, D. Rush, Cone calorimeter tests of combustible materials found in informal
835 settlements, [dataset], (2019). <https://doi.org/10.7488/ds/2599>.
- 836 24. D. Rush, L. Gibson, G. Bankoff, R. Walls, G. Spinardi, S. Cooper-Knock, J. Twigg, E. Al., Fire
837 Risk Reduction in an Urbanizing World, in: United Nations Off. Disaster Risk Reduct.,
838 Geneva, 2019.
- 839 25. R. Walls, P. Zweig, Towards sustainable slums : understanding fire engineering in informal
840 settlements, Sustain. Vital Technol. Eng. Informatics. (2016) 1–5.
- 841 26. G. Baker, M. Spearpoint, C.. Fleischmann, C. Wade, Selecting an ignition criterion
842 methodology for use in a radiative fire spread submodel, Fire Mater. 35 (2011) 367–381.
843 <https://doi.org/10.1002/fam.1059>.
- 844 27. V. Babrauskas, Heat release rates, in: M.J. Hurley et. al (Ed.), SFPE Handb. Fire Prot. Eng., 5th
845 ed., Springer, 2016: p. 829. <https://doi.org/10.1007/978-1-4939-2565-0>.
- 846 28. A. Cicione, R. Walls, Estimating time to structural collapse of informal settlement dwellings
847 based on structural fire engineering principles, in: SEMC Conf., CRC Press, 2019.
- 848 29. R.S. Walls, P. Zweig, Towards sustainable slums: understanding fire engineering in informal
849 settlements, in: Y. Bahei-El-Din, M. Hassan (Eds.), Adv. Technol. Sustain. Syst., Springer,
850 Cairo, 2017: pp. 93–98. <https://doi.org/10.1007/978-3-319-48725-0>.
- 851 30. K. Mcgrattan, R. Mcdermott, H. Simo, J. Floyd, M. Vanella, C. Weinschenk, K. Overholt, Fire
852 Dynamics Simulator Technical Reference Guide Volume 3 : Validation, NIST Spec. Publ. 1018-
853 3. 3 (2017).
- 854 31. Y. Wang, L. Gibson, M. Beshir, D. Rush, Preliminary investigation of critical separation
855 distance between shacks in informal settlements fire, in: 11th Asia-Oceania Symp. Fire Sci.
856 Technol., 2018.
- 857 32. L. Gibson, A. Adeleke, R. Hadden, D. Rush, Spatial metrics from LiDAR roof mapping for fire
858 spread risk assessment of informal settlements in Cape Town, South Africa., Fire Saf. J. (n.d.).
- 859 33. University of Edinburgh. School of Engineering. Infrastructure and Environment., Dwelling
860 outline - Informal Settlements of Cape Town, 2018 [dataset], (2020).
861 <https://doi.org/10.7488/ds/2758> (accessed December 3, 2020).
- 862 34. D.C. Montgomery, C.L. Jennings, M. Kulahci, Introduction Time Series Analysis and
863 Forecasting, Wiley, 2016.
- 864 35. L. Gibson, Informal dwelling fires, 2009 - 2015, City of Cape Town, 2009-2015 [dataset]. School
865 of Engineering, University of Edinburgh., (2020).
- 866 36. S. Stevens, L. Gibson, D. Rush, Conceptualising a GIS-based risk quantification framework for
867 fire spread in informal settlements: A Cape Town case study, Int. J. Disaster Risk Reduct.
868 (n.d.).
869



© 2020 by the authors. Submitted for possible open access publication under the terms and conditions of the Creative Commons Attribution (CC BY) license (<http://creativecommons.org/licenses/by/4.0/>).